

Alignment and Comparison of Directed Networks via Transition Couplings of Random Walks

Bongsoo Yi*
UNC-Chapel Hill

Kevin O'Connor*
UNC-Chapel Hill

Kevin McGoff
UNC-Charlotte

Andrew B. Nobel†
UNC-Chapel Hill

December 29, 2022

Abstract

We introduce and analyze NetOTC, a procedure for the comparison and soft alignment of weighted networks. Given two networks and a cost function relating their vertices, NetOTC finds an appropriate coupling of their associated random walks having minimum expected cost. The minimizing cost provides a numerical measure of the difference between the networks, while the optimal transport plan itself provides interpretable, probabilistic alignments of the vertices and edges of the two networks. The cost function employed can be based, for example, on vertex degrees, externally defined features, or Euclidean embeddings. Coupling of the full random walks, rather than their stationary distributions, ensures that NetOTC captures local and global information about the given networks. NetOTC applies to networks of different size and structure, and does not require specification of free parameters. NetOTC respects edges, in the sense that vertex pairs in the given networks are aligned with positive probability only if they are adjacent in the given networks.

We investigate a number of theoretical properties of NetOTC that support its use, including metric properties of the minimizing cost and its connection with short- and long-run average cost. In addition, we introduce a new notion of factor for weighted networks, and establish a close connection between factors and NetOTC. Complementing the theory, we present simulations and numerical experiments showing that NetOTC is competitive with, and sometimes superior to, other optimal transport-based network comparison methods in the literature. In particular, NetOTC shows promise in identifying isomorphic networks using a local (degree-based) cost function.

Keywords: Graph alignment, Graph comparison, Optimal transport, Graph factor

*Bongsoo Yi and Kevin O'Connor are co-first authors for the paper.

†Corresponding author; E-mail: nobel@email.unc.edu

1 Introduction

Networks have long been used as a means of representing and studying the pairwise interactions between a set of individuals or objects under study. More recently, networks themselves have become objects of study. Networks appear as data objects in a number of applications, including comparing protein interaction networks [73, 40, 42, 26], aligning single-cell multi-omics data [19], deanonymizing private networks [61, 62, 70], pattern recognition [11, 5, 53], image captioning [9, 87], and language comparison [3].

Analysis of network-based data often begins with network alignment or comparison, tasks that have been studied in a number of fields. In the simplest version of the network alignment problem, one is given two networks with vertex sets of equal size and seeks to find a bijection between the vertex sets that maximizes the number of aligned edges. Numerous approaches to network alignment have been considered in the literature, e.g. [41, 47, 48, 39, 44]. By contrast, the goal of network comparison is to identify quantitative differences between weighted networks of different sizes or structures. Networks of this sort may arise from distinct data sets or scientific domains.

In this paper, we propose and analyze Network Comparison and Alignment using Optimal Transition Coupling (NetOTC), a flexible procedure for the comparison and soft alignment of weighted networks that is based on a process-level version of optimal transport. The NetOTC procedure takes as input two connected networks G_1 and G_2 with non-negative edge weights, and a cost function relating their vertices. Each network gives rise to a random walk on its vertex set, which is a stationary Markov chain. NetOTC proceeds by finding a coupling of these Markov chains (a transport plan) that is itself stationary and Markov, and that minimizes the expected value of the cost function at any given time point. (For computational and theoretical reasons discussed below, NetOTC considers a sub-family of Markov couplings known as transition couplings.) The optimal transport plan is a stationary random walk on the product of the vertex sets of the given networks that favors low cost pairs, while maintaining the marginal structure of the random walks on each individual network.

The cost function used in NetOTC is specified by the user, and will, in general, be application dependent. Cost functions can be based, for example, on the difference between externally specified vertex attributes, the distance between Euclidean embeddings of the vertices, and the difference between the degrees of the vertices. If the given networks have the same vertex set, a cost function based on vertex identity may be used as well.

The NetOTC procedure has a number of desirable methodological and theoretical properties. On the methodological side, NetOTC applies to directed and undirected networks, and readily handles networks with different sizes and connectivity structures. As NetOTC considers process-level couplings of random walks, the optimal transport plan captures global information reflected in the stationary distributions of the random walks, as well as local information that is present in the transition probabilities between vertices. The expected cost of the optimal transport plan provides a numerical measure of the difference between the networks. The distribution of the optimal transport plan at a single time point yields a soft, probabilistic alignment of the vertices in the given networks. Moreover, the distribution of the optimal transport plan at two successive time points yields a soft, probabilistic alignment of the *edges* of the given networks. To the best of our knowledge, native alignment of edges is unique to NetOTC among existing alignment and comparison methods. The exact version of the NetOTC procedure has no free parameters and is not randomized.

On the theoretical side, we establish several key properties of the NetOTC procedure that support its use in comparison and alignment tasks. The edge alignment of NetOTC respects edges, in the sense that vertex pairs in the given networks are aligned with positive probability only if each pair is connected by an edge in its respective network. Although the NetOTC optimal transport plan minimizes the expected cost between vertices at a single time point, stationarity ensures that the coupled random walk has a low average cost between vertices across time. The NetOTC similarity measure is sensitive to differences in the k -step behavior of the random walks on G_1 and G_2 if these differences affect the cumulative cost. For undirected networks with a common vertex set, the NetOTC similarity is a metric on equivalence classes of networks having identical random walks if the cost c is a metric. For the zero-one cost, the NetOTC similarity is lower bounded by the L_1 -difference of the network degree sequences, and the L_1 -difference of the network weight functions.

In addition, we study the structure of the NetOTC method through network factors. Our definition of factor, which arises naturally when considering functions of Markov chains, differs from other definitions in the network theory literature. Informally, a network G_2 is a factor of a network G_1 if the vertices of G_2 can be associated, via a vertex map f , with disjoint sets of vertices in G_1 between which aggregate weights can be consistently defined. If G_2 is a factor of G_1 we show that the vertex map f yields a deterministic transition coupling of their associated random walks. Under suitable compatibility conditions on the cost function, this coupling will be optimal and will provide a solution to the NetOTC problem. The resulting expected cost, vertex and edge alignments are fully determined by the structure of G_1 and the map f . Importantly, the existence and precise nature of the map f need not be known to the NetOTC procedure. These results extend to paired factors: an optimal transition coupling for a pair of networks can be mapped in a deterministic fashion to an optimal transition coupling of their factors when

the cost functions for each pair are compatible with the factor maps.

As a complement to the theory, we carry out a number of simulations and numerical experiments to assess the performance of NetOTC and compare it with other optimal transport-based comparison methods in the literature. NetOTC is competitive with other methods on a number of network classification tasks. In an extensive experiment on pairs of isomorphic networks with small to moderate sizes, NetOTC was consistently able to recover the isomorphism using a local (degree-based) cost function, substantially outperforming other methods. When applied to stochastic block models (with equivalent blocks of different sizes) using a degree-based cost function, NetOTC was competitive with other methods in its ability to align vertices in equivalent blocks, and substantially better at aligning edges. We also considered the problem of comparing a network to an exact or approximate factor using a distance-based cost derived from Euclidean vertex embeddings of the given networks. NetOTC outperforms other methods in its ability to align vertices in the parent and factor networks. While the performance gap is modest for exact factors, it increases as one considers approximate factors.

1.1 Outline of the Paper

The next section gives an overview of existing work on optimal transport and related approaches to network comparison and alignment. Section 3 provides background concerning random walks on directed networks, optimal transport for Markov chains, and transition couplings. The NetOTC procedure is described in Section 4, including computation, the optimal transport cost, and vertex and edge alignment. Section 5 is devoted to the formal statement and discussion of the theoretical properties of NetOTC. Proofs are given in Section 7. Section 6 contains a number of simulations and a number of experiments that demonstrate the flexibility and potential utility of NetOTC. Additional details concerning the experiments are given in Appendix A.

2 Related Work

The problems of network alignment and comparison have received a lot of recent attention in the literature. Approaches using optimal transport ideas can be divided into two groups: spectral and variants of Gromov-Wasserstein. Other approaches make use of quadratic programming and continuous approximations. This related work is discussed below.

Spectral Methods. One line of work [21, 57, 58] uses techniques from spectral graph theory to define optimal transport (OT) problems for networks. In particular, this approach associates to each network a multivariate Gaussian with zero mean and covariance matrix equal to the pseudo-inverse of the graph Laplacian. The Wasserstein distance between Gaussian distributions of the same dimension may be computed analytically in terms of their respective covariance matrices. For networks with different numbers of vertices, [58] and [21] propose to optimize this distance over soft many-to-one assignments between vertices in either network. At present, this family of approaches is unable to incorporate available feature information or underlying cost functions, relying only on their intrinsic structure.

Variants of Gromov-Wasserstein. Another line of work [60, 68, 76, 81, 80] considers the Gromov-Wasserstein (GW) distance and related extensions. In this work, one tries to couple distributions on the vertices in each network so as to minimize an expected transport cost between vertices while minimizing changes in edges between the two networks. This approach allows one to capture differences in both features and structure between networks. We refer the reader to [21] for a discussion on the differences between spectral-based network OT methods and GW distances. A number of variants of the GW distance have been proposed for a variety of tasks including cross-domain alignment [9], graph partitioning [83], graph matching [83, 84], and node embedding [84]. The work [7] proposes to incorporate global structure into the Wasserstein and Fused GW (FGW) distances by applying a heat diffusion to the vertex features before computing the cost matrix.

Other Methods for Network Alignment and Comparison. There is also a large body of work devoted to network alignment and comparison that do not use optimal transport methods. The network alignment problem can be generally defined as a quadratic programming problem under discrete and doubly stochastic constraints [85, 38, 55, 10, 13]. However, as the optimal network alignment problem is well known to be an NP-hard problem [30], it is computationally challenging to obtain an optimal alignment for networks. For this reason, many authors have proposed approximate solutions for network alignment [10, 92, 89, 27, 79, 90]. Among these approximate methods, most of the successful algorithms start with relaxing the discrete constraints to create a continuous

condition. Several authors [72, 78] relax the discrete conditions to form a positive semi-definite problem. A non-convex quadratic programming problem was adopted in [32, 10, 92]. In another direction, [50] introduces spectral matching as a simple relaxation, and [13] strengthens this approach by giving an affine constraint. Also, [38] proposes an algorithm that can efficiently solve a general quadratic programming problem with doubly stochastic constraints. Each step of the algorithm is easy to implement and the convergence is guaranteed. Generally, after finding the optimal solution for the relaxed continuous problem, the discrete alignment is attained through a final discretization process [10, 50, 51]. We note that these approaches may find a solution that is locally optimal but not globally optimal.

There is also a line of research devoted to the statistical and probabilistic analysis of graph matching when the given graphs are generated at random but are correlated with one another, e.g., each is a random perturbation of a given graph [20, 6, 15, 14, 28, 45, 56, 88]. Much of this work investigates various matching procedures under specific random graph models, such as correlated Erdos-Renyi graphs, and is concerned with the information-theoretic threshold for exact recovery, and the time complexity of the matching procedures.

3 Transition Couplings of Random Walks on Networks

This section provides background for the detailed description of the NetOTC procedure. We begin by recalling how a weighted network gives rise to a random walk on its vertex set and reviewing the definition and framework of optimal transport. We then consider transition couplings of random walks, which preserve stationarity and the Markov property. The computation of optimal transition couplings is the basis for the NetOTC procedure, which is described in Section 4 below.

3.1 Random Walks on Directed Networks

Let $G = (U, E, w)$ denote a weighted directed network with finite vertex set U , edge set $E \subseteq U \times U$, and non-negative weight function $w : U \times U \rightarrow \mathbb{R}_+$. An ordered pair $(u, u') \in E$ denotes a directed edge from u to u' . We assume in what follows that $w(u, u') > 0$ if and only if $(u, u') \in E$. For any vertex $u \in U$, we let $d(u) = \sum_{u' \in U} w(u, u')$ be the weighted out-degree of u . An undirected network may be represented by a directed network in which $w(u, u') = w(u', u)$. A path in G is an ordered sequence of vertices $u_0, \dots, u_n \in U$ such that $(u_i, u_{i+1}) \in E$ for each $i = 0, \dots, n-1$. A network G is strongly connected if for each ordered pair $(u, v) \in U \times U$ there exists a path u_0, \dots, u_n in G such that $u_0 = u$ and $u_n = v$.

To any network $G = (U, E, w)$, one may associate a Markov transition kernel $P(\cdot | \cdot)$ with state space U as follows. Given states u and u' in U , the probability of transitioning from u to u' is

$$P(u' | u) = \frac{w(u, u')}{\sum_{\tilde{u} \in U} w(u, \tilde{u})}.$$

Recall that a probability distribution p on U is said to be stationary for $P(\cdot | \cdot)$ if

$$p(u') = \sum_{u \in U} p(u) P(u' | u), \quad \forall u' \in U.$$

The transition kernel $P(\cdot | \cdot)$ admits at least one stationary distribution. When G is strongly connected the kernel $P(\cdot | \cdot)$ admits a *unique* stationary distribution. The transition kernel P and a stationary distribution p together define a stationary Markov chain on U , denoted by $X = X_0, X_1, X_2, \dots$, where for any u_0, \dots, u_n in U we have

$$\mathbb{P}(X_0 = u_0, \dots, X_n = u_n) = p(u_0) \prod_{i=0}^{n-1} P(u_{i+1} | u_i).$$

The Markov chain X is commonly referred to as a random walk on G . When G is strongly connected, we may refer to X as *the* random walk on G . Random walks on networks have been studied extensively in the probability literature, and have found numerous applications in fields ranging from genomics to computer science, including recent work on network embedding [35, 34, 66]. In what follows, we will generally assume that the networks under consideration are strongly connected. In this case, we note that the random walk X on G is an irreducible Markov chain.

3.2 Optimal Transport

Let X and Y be random variables taking values in measurable spaces $(\mathcal{X}, \mathcal{A})$ and $(\mathcal{Y}, \mathcal{B})$ respectively. Recall that a *coupling* of X and Y is a jointly distributed pair of random variables (\tilde{X}, \tilde{Y}) taking values in $(\mathcal{X} \times \mathcal{Y}, \mathcal{A} \times \mathcal{B})$ such that $\tilde{X} \stackrel{d}{=} X$ and $\tilde{Y} \stackrel{d}{=} Y$. Couplings have been widely studied in the probability literature, and are the basic objects of interest in optimal transport. Let $\Pi(X, Y)$ denote the set of all couplings of X and Y . Note that $\Pi(X, Y)$ is not empty, as it always contains the independent coupling of X and Y . Each coupling $(\tilde{X}, \tilde{Y}) \in \Pi(X, Y)$ can be viewed as a plan for transporting the distribution of X to that of Y , or vice versa.

Now let $c : \mathcal{X} \times \mathcal{Y} \rightarrow \mathbb{R}_+$ be a measurable, non-negative cost function relating the elements of \mathcal{X} and \mathcal{Y} . The optimal transport problem is to minimize the expected value of the cost over all couplings of X and Y , namely

$$\text{minimize } \mathbb{E}c(\tilde{X}, \tilde{Y}) \text{ over } (\tilde{X}, \tilde{Y}) \in \Pi(X, Y).$$

A minimizer of the optimal transport problem is called an optimal coupling of X and Y , or an optimal transport plan. The theory and applications of optimal transport are active areas of research. See [67, 82] for further reading and more details.

3.3 Transition Couplings

Let $G_1 = (U, E_1, w_1)$ and $G_2 = (V, E_2, w_2)$ be weighted directed networks, and let $c : U \times V \rightarrow \mathbb{R}_+$ be a cost function relating their vertex sets. As described above, the network G_1 is associated with a random walk $X = X_0, X_1, \dots$ on the vertex set U . We may regard the process X as a random element of the set $\mathcal{X} = U^{\mathbb{N}}$ equipped with the Borel sigma-field arising from the usual product topology on $U^{\mathbb{N}}$. Similarly, the network G_2 is associated with a random walk $Y = Y_0, Y_1, \dots$ taking values in $\mathcal{Y} = V^{\mathbb{N}}$. Note that a coupling of the processes X and Y is a joint process

$$(\tilde{X}, \tilde{Y}) = (\tilde{X}_0, \tilde{Y}_0), (\tilde{X}_1, \tilde{Y}_1), (\tilde{X}_2, \tilde{Y}_2), \dots$$

such that $\tilde{X} = \tilde{X}_0, \tilde{X}_1, \dots \stackrel{d}{=} X$ and $\tilde{Y} = \tilde{Y}_0, \tilde{Y}_1, \dots \stackrel{d}{=} Y$. A coupling of X and Y need not be stationary or Markov, an issue that we take up below.

In order to address optimal transport of the full random walks X and Y , we first extend the cost function c to $\mathcal{X} \times \mathcal{Y}$ by setting $\tilde{c}(x, y) = c(x_0, y_0)$. The standard optimal transport problem with cost \tilde{c} seeks to minimize $\mathbb{E}c(\tilde{X}_0, \tilde{Y}_0)$ over the family $\Pi(X, Y)$ of all couplings of the Markov chains X and Y . However, for most purposes, the family $\Pi(X, Y)$ is too large: in general, it will include couplings that are non-stationary, and not Markov of any order. Moreover, an optimal coupling will minimize the expected cost only at time zero, after which the processes \tilde{X} and \tilde{Y} may evolve independently (and potentially have a large realized cost). Restricting attention to stationary couplings addresses some of these issues [64, 63], but it is natural to go further and consider only couplings (\tilde{X}, \tilde{Y}) that are themselves first order Markov chains, that is, couplings whose structure matches that of the constituent processes. Stationary couplings of stationary processes, also known as joinings, have been widely studied in the ergodic theory literature (see [16, 31, 65] and the references therein).

Unfortunately, even the family of first order Markov couplings presents some difficulties: there is no fast method for computing optimal couplings, and the optimal expected cost need not have the properties of a metric even when the cost c does [22, 23]. For these reasons, we restrict attention to the subfamily of transition couplings.

Definition 1. Let X be a stationary U -valued Markov chain with transition kernel P , and let Y be a stationary V -valued Markov chain with transition kernel Q . A stationary Markov chain (\tilde{X}, \tilde{Y}) on the state space $U \times V$ is a transition coupling of X and Y if it is a coupling of X and Y and if it has a transition kernel R such that for every $u, u' \in U$ and $v, v' \in V$,

$$\sum_{\tilde{v} \in V} R(u', \tilde{v} \mid u, v) = P(u' \mid u), \quad \text{and} \quad \sum_{\tilde{u} \in U} R(\tilde{u}, v' \mid u, v) = Q(v' \mid v). \quad (1)$$

Let $\Pi_{TC}(X, Y)$ denote the set of all transition couplings of X and Y .

The transition coupling condition (1) can be stated equivalently as follows: for every $u \in U$ and $v \in V$ the conditional distribution $R(\cdot \mid u, v)$ of the joint chain is a coupling of the conditional distributions $P(\cdot \mid u)$ and $Q(\cdot \mid v)$ of the chains X and Y . The set of transition couplings $\Pi_{TC}(X, Y)$ is non-empty, as the independent coupling of X and Y , with transition kernel $R(u', v' \mid u, v) = P(u' \mid u) Q(v' \mid v)$, is a transition coupling. Further examples of transition couplings can be found in Chapter 5 of [52].

4 NetOTC

In this section, we describe the NetOTC procedure in more detail, including a statement of the NetOTC problem, as well as exact and approximate computational methods for its solution.

4.1 The NetOTC Problem

Let G_1 and G_2 be given strongly connected networks with associated random walks X and Y . The NetOTC problem seeks to minimize $\mathbb{E}c(\tilde{X}_0, \tilde{Y}_0)$ over all transition couplings (\tilde{X}, \tilde{Y}) of X and Y . In particular, we wish to identify both the minimizing value

$$\rho(G_1, G_2) = \min_{(\tilde{X}, \tilde{Y}) \in \Pi_{\text{TC}}(X, Y)} \mathbb{E}c(\tilde{X}_0, \tilde{Y}_0), \quad (2)$$

and an associated optimal transition coupling

$$(X^*, Y^*) \in \underset{(\tilde{X}, \tilde{Y}) \in \Pi_{\text{TC}}(X, Y)}{\operatorname{argmin}} \mathbb{E}c(\tilde{X}_0, \tilde{Y}_0). \quad (3)$$

As noted above, the set $\Pi_{\text{TC}}(X, Y)$ of transition couplings is non-empty. We endow $\Pi_{\text{TC}}(X, Y)$ with the standard topology (inherited as a subset of the weak* topology on the space of finite-valued stochastic processes) under which it is compact and the expected cost function $(\tilde{X}_0, \tilde{Y}_0) \mapsto \mathbb{E}c(\tilde{X}_0, \tilde{Y}_0)$ is continuous. Thus, the minimum in (2) is achieved, and there exists an optimal transition coupling in (3). In general, there may be many solutions to the NetOTC problem. For example, if the cost function is constant, then all transition couplings are optimal.

While the objective function of the NetOTC problem involves only the first time point of the joint process (\tilde{X}, \tilde{Y}) , the restriction to stationary processes ensures that the optimal transition coupling performs well on average over multiple time points (see Proposition 4 below). Moreover, the transition coupling constraint further restricts the set of allowable couplings: in general, the minimizing value of $\mathbb{E}c(\tilde{X}_0, \tilde{Y}_0)$ will (strictly) decrease as one moves from transition couplings to general Markov couplings, from Markov couplings to stationary couplings, and from stationary couplings to general couplings [22, 23, 25, 24, 64, 63].

It is important to note that the NetOTC problem is *not* equivalent to finding a one-step optimal transition coupling [74, 91]. In the latter problem one finds, for every $u \in U$ and $v \in V$, a coupling $(\tilde{X}_0, \tilde{Y}_0)$ of $X_0 \sim P(\cdot|u)$ and $Y_0 \sim Q(\cdot|v)$ minimizing $\mathbb{E}c(\tilde{X}_0, \tilde{Y}_0)$. The one-step optimal transition coupling does not ensure good performance over multiple time steps, as it does not account for the global structure of the given networks.

4.2 Computation of NetOTCs

Solving the NetOTC problem requires finding an optimal transition coupling (OTC) for the random walks X and Y on G_1 and G_2 . Although this problem is non-convex, it was shown in [64] that one can find OTCs by combining ideas from reinforcement learning and computational optimal transport. In particular, one may obtain OTCs via an adaptation of the policy iteration algorithm [37], which is referred to as `ExactOTC`. The `ExactOTC` algorithm requires $\mathcal{O}((|U||V|)^3)$ operations per iteration. In practice, the algorithm converges after fewer than 5 iterations. A more efficient algorithm, `EntropicOTC`, based on entropic regularization and Sinkhorn iterations was also proposed in [64]. When applied to NetOTC, the `EntropicOTC` algorithm requires $\mathcal{O}((|U||V|)^2)$ operations per iteration (up to poly-logarithmic factors), which is nearly-linear in the dimension of the couplings under consideration, and in this sense comparable to the state-of-the-art for entropic OT algorithms [67]. The current implementation of NetOTC can handle networks with up to 200 vertices. Research on faster computation of OTCs is currently ongoing.

As noted above, the NetOTC problem may have multiple solutions. The `ExactOTC` algorithm is only guaranteed to return a single minimizer, which is not guaranteed to be irreducible. On the other hand, the entropically regularized problem solved by `EntropicOTC` has a unique minimizer, which is aperiodic and irreducible when X and Y are aperiodic and irreducible.

4.3 Cost Functions

In practice, the specification of a cost function depends on the goals of the network alignment or comparison problem. The cost function is typically based on prior information about the vertex sets of the given networks, including vertex features and embeddings, if these are available. If $U = V$ we may use the 0-1 cost $c(u, v) = \mathbb{I}(u \neq v)$. If the vertices of G_1 and G_2 are associated with features or attributes in a common, discrete set \mathcal{S} then one may take $c(u, v) = \rho(\tilde{u}, \tilde{v})$ where ρ is a cost function relating the elements of \mathcal{S} , and $\tilde{u}, \tilde{v} \in \mathcal{S}$ are the features associated

with vertices u and v , respectively. If \mathcal{S} is a finite set, the zero-one cost $c(u, v) = \mathbb{I}(\tilde{u} \neq \tilde{v})$ is often a good choice. If the vertices of G_1 and G_2 are embedded in a common Euclidean space \mathbb{R}^d via embeddings $h_1 : U \rightarrow \mathbb{R}^d$ and $h_2 : V \rightarrow \mathbb{R}^d$, then it is natural to use an embedding-based cost such as $c(u, v) = \|h_1(u) - h_2(v)\|$ or $c(u, v) = \|h_1(u) - h_2(v)\|^2$. In cases where such prior maps are unavailable, one may consider costs defined in terms of intrinsic properties of the networks of interest, or embed the vertices in a Euclidean space a priori using methods such as Laplacian eigenmaps [8].

A cost function that is applicable in general is the degree-based cost: $c(u, v) = (\deg(u) - \deg(v))^2$. For undirected networks, $\deg(u)$ is sum of weights of all edges adjacent to u . For directed networks, one may use in-degree, out-degree, or a combination of these. Unless otherwise specified, we use out-degree in this paper. One may also use the standardized degree $\bar{d}(u) = \deg(u) / \sum_{u' \in U} \deg(u')$ when comparing networks of significantly different sizes. Extending this idea, one may employ cost $c(u, v)$ based on the degree distributions of a fixed local neighborhood of u and v .

4.4 NetOTC Deliverables

Every strongly connected directed network gives rise to a unique random walk on its vertex set, whose transition probabilities are determined by the connectivity and edge weights of the network. The stationary distribution and transition probabilities of the random walk reflect the global and local structure of the network, respectively. Let X and Y be the random walks associated with networks G_1 and G_2 , respectively. The optimal transport plan identified by NetOTC corresponds to an optimal transition coupling, which can be represented as a stationary random walk

$$(X^*, Y^*) = (X_0^*, Y_0^*), (X_1^*, Y_1^*), \dots$$

on the product $U \times V$ that preserves the marginal behavior of the walks X and Y , while favoring pairs u, v with low cost. Note again that (X^*, Y^*) is an optimal coupling of the *processes* X and Y , not their one-dimensional (stationary) distributions. As such, the optimal transport plan identified by NetOTC captures, and links, the local and global structure of the given networks. The NetOTC procedure does not rely on randomization; its output is fully determined by the given networks and the cost function c . When it makes use of the `ExactOTC` algorithm, the NetOTC procedure has no free parameters.

Difference measure for networks. The solution of the NetOTC problem yields the minimizing value $\rho(G_1, G_2)$ of the expected cost, and the associated optimal transition plan (X^*, Y^*) . The minimum cost $\rho(G_1, G_2)$ measures the difference between G_1 and G_2 and can be utilized for network comparison tasks. For undirected networks with the same vertex set, $\rho(\cdot, \cdot)$ is a metric if the cost function is a metric (see Proposition 8).

Vertex alignment. The optimal transport plan (X^*, Y^*) itself provides soft, probabilistic alignments of the vertices and edges of G_1 and G_2 based on the joint distribution of pairs in the coupled chain. The vertex alignment π_v produced by NetOTC is derived from the stationary distribution of the optimal transport plan (X^*, Y^*) , which is the distribution of the pair (X_0^*, Y_0^*) . For $u \in U$ and $v \in V$ define the vertex alignment

$$\pi_v(u, v) = \mathbb{P}((X_0^*, Y_0^*) = (u, v)).$$

One may define probabilistic vertex alignments in a similar manner for other OT-based network comparison methods (see Section 6.3 and 6.4).

Edge alignment. A unique feature of NetOTC is that the optimal transport plan naturally yields a probabilistic alignment of the edges of the given networks. The edge alignment is obtained from the first two pairs $\{(X_0^*, Y_0^*), (X_1^*, Y_1^*)\}$ in the optimal transport plan. For $u, u' \in U$ and $v, v' \in V$ define the edge alignment

$$\pi_e((u, u'), (v, v')) = \mathbb{P}((X_0^*, Y_0^*) = (u, v), (X_1^*, Y_1^*) = (u', v')).$$

It is straightforward to show (see Proposition 2) that vertex pairs aligned with positive probability must be adjacent in their respective networks. In other words, NetOTC aligns only existing edges; it does not create new ones. By contrast, most alignment methods in the literature have as their primary focus the matching of vertices, with edges functioning primarily as a means of evaluating matchings. Alignments arising in this way can map adjacent vertices in G_1 to non-adjacent vertices in G_2 , or vice versa.

5 Theoretical Properties of NetOTC

In this section, we explore some theoretical properties of NetOTC, beginning with the edge-alignment property and several results concerning the behavior of NetOTC under average cost criteria. For undirected networks with a

common vertex set, we establish that the NetOTC cost has the properties of a metric when the cost c does, and we investigate the sensitivity of NetOTC to local information arising from degree and weight functions. We then define a notion of *network factor* that captures the idea of one network being “folded” or “compressed” to produce another. Although the literature contains several definitions of network factors or factor networks, the definition given here appears to be new. We establish a close connection between factors and transition couplings, and then we present two results describing the behavior of NetOTC in the presence of this type of network factor structure. All proofs of the results in this section may be found in Section 7.

5.1 NetOTC Edge Alignment

The NetOTC edge alignment function π_e respects edges, in the sense that vertex pairs aligned with positive probability must be adjacent in the given networks.

Proposition 2. *Let π_e be the NetOTC edge alignment of networks $G_1 = (U, E_1, w_1)$ and $G_2 = (V, E_2, w_2)$ based on the optimal transport plan (X^*, Y^*) . If $\pi_e((u, u'), (v, v')) > 0$ then $(u, u') \in E_1$ and $(v, v') \in E_2$.*

5.2 NetOTC and Multistep Cost

The NetOTC cost $\rho(G_1, G_2)$ is the expected cost $\mathbb{E}c(\tilde{X}_0, \tilde{Y}_0)$ at the initial state of the optimal transport plan. Here we consider the average cost of the optimal transport plan over multiple time points, which provides insights into the behavior of NetOTC.

Definition 3. *For an infinite sequence x_0, x_1, \dots and integers $0 \leq i \leq j$ let $x_i^j = (x_i, \dots, x_j)$. For each $k \geq 1$ define the k -step average cost $c_k(x_0^{k-1}, y_0^{k-1}) = k^{-1} \sum_{j=0}^{k-1} c(x_j, y_j)$ and the limiting average cost $\bar{c}(x, y) = \limsup_{k \rightarrow \infty} c_k(x_0^{k-1}, y_0^{k-1})$.*

Stationarity ensures that the NetOTC problem is equivalent to minimizing the long-term average cost over the set of transition couplings.

Proposition 4. *Let G_1 and G_2 be networks with associated random walks X and Y . Then*

$$\rho(G_1, G_2) = \min_{(\tilde{X}, \tilde{Y}) \in \Pi_{\text{TC}}(X, Y)} \mathbb{E}\bar{c}(\tilde{X}, \tilde{Y}),$$

and the optimal transport plans minimizing $\mathbb{E}\bar{c}(\tilde{X}, \tilde{Y})$ coincide with those minimizing $\mathbb{E}c(\tilde{X}_0, \tilde{Y}_0)$.

The long-term behavior of the random walks X and Y encodes information about the global structure of the networks G_1 and G_2 , respectively. The next result shows that NetOTC also captures local information arising from the finite time behavior of the walks X and Y . For example, if G_1 and G_2 are distinguishable based on optimal transport of their k -step random walks, then they are distinguishable by NetOTC.

Proposition 5. *Let G_1 and G_2 be networks with associated random walks X and Y . For each $k \geq 1$*

$$\rho(G_1, G_2) \geq \min \mathbb{E} c_k(\tilde{X}_0^{k-1}, \tilde{Y}_0^{k-1}),$$

where the minimum is over the family of all couplings of X_0^{k-1} and Y_0^{k-1} .

5.3 Undirected Networks with a Common Vertex Set

In this section, we consider undirected networks $G_1 = (U, E_1, w_1)$ and $G_2 = (U, E_2, w_2)$ with the same vertex set, but potentially different edge sets and weight functions. We assume throughout that the networks are connected. We begin by defining a natural equivalence relation on such networks.

Definition 6. *Undirected networks G_1 and G_2 are equivalent, denoted by $G_1 \sim G_2$, if they have the same vertex U , the same edge set E , and there exists a constant $C > 0$ such that $w_1(u, u') = C w_2(u, u')$ for every $u, u' \in U$.*

The following result relates the equivalence of networks to their random walks.

Proposition 7. *Connected undirected networks G_1 and G_2 are equivalent if and only if their respective random walks are identical.*

Whatever the underlying cost c , the cost $\rho(G_1, G_2)$ and optimal transport plan arising from NetOTC depend only on the equivalence classes of the networks G_1 and G_2 . In particular, NetOTC is invariant under (positive) scaling of weight functions. When the underlying cost c is a metric on U , the NetOTC cost is a metric on these equivalence classes.

Proposition 8. *If the cost function $c : U \times U \rightarrow \mathbb{R}_+$ satisfies the properties of a metric on U , then ρ is a metric on the equivalence classes of undirected networks with vertex set contained in U defined by \sim .*

We now investigate the sensitivity of NetOTC to differences between the degree and weight functions of the given networks.

Definition 9. *The degree function of an undirected network $G = (U, E, w)$ is given by $d(u) = \sum_{u' \in U} w(u, u')$ for $u \in U$. Let $D = \sum_{u \in U} d(u)$ denote the total degree of G .*

The next proposition strengthens the general result of Proposition 5.

Proposition 10. *Let G_1 and G_2 be undirected networks with the same vertex set. Let $d_1(u)$ and $d_2(u)$ be the degree functions of G_1 and G_2 , respectively, and assume that each network has total degree D . Then under the zero-one cost $c(u, u') = \mathbb{I}(u \neq u')$,*

$$\begin{aligned} \bullet \quad \rho(G_1, G_2) &\geq \frac{1}{2D} \sum_{u \in U} |d_1(u) - d_2(u)| \\ \bullet \quad \rho(G_1, G_2) &\geq \frac{1}{4D} \sum_{u, u' \in U} |w_1(u, u') - w_2(u, u')| \end{aligned}$$

5.4 Deterministic Transition Couplings and Factor Maps

The graph theory and network literature contain several definitions of “network factor” and “factor network”. A network factor of G is often defined to be any spanning subnetwork of G , while the term factor network is used in the context of message passing algorithms and error-correcting codes to refer to a bipartite network that captures the factorization of a function or a probability distribution. Here we define a notion of network factor that appears to be different than existing definitions in the literature, see for example the survey [69]. We show that there is a close connection between factors and transition couplings, and we use this to rigorously study the behavior of NetOTC when factor structure is present. Our results establish a close link between NetOTC and factors, behavior that distinguishes NetOTC from other comparison and alignment methods.

Definition 11. *Let $G_1 = (U, E_1, w_1)$ and $G_2 = (V, E_2, w_2)$ be strongly connected, weighted directed networks with out-degree functions d_1 and d_2 , respectively. A map $f : U \rightarrow V$ is a factor map if for all $v, v' \in V$ and $u \in f^{-1}(v)$,*

$$\sum_{u' \in f^{-1}(v')} w_1(u, u') = \frac{d_1(u)}{d_2(v)} w_2(v, v'). \quad (4)$$

In this case, we will say that G_2 is a factor of G_1 , and that G_1 is an extension of G_2 .

Example 12. *Consider the networks G_1 and G_2 drawn in Figure 1 with vertices embedded in \mathbb{R}^2 . G_2 is a factor of G_1 with respect to the map f that takes $(-1, 1)$ and $(-1, -1)$ to $(-1, 0)$, $(0, 0)$ to $(0, 0)$, and $(1, 0)$ and $(1, -1)$ to $(1, 0)$.*

The definition of factor arises naturally from the random walk perspective. If G_1 and G_2 have associated random walks X and Y , and G_2 is a factor of G_1 under the map f , then the process $f(X) := f(X_1), f(X_2), \dots$ is equal in distribution to Y , see Theorem 15 below for more details. Factors have been well studied in ergodic theory and symbolic dynamics. The existence of a factor map (in the sense above) ensures that Y is a stationary coding of X , which is a special case of a factor relationship in ergodic theory. Moreover, if G_2 is a factor of G_1 , then the subshift of finite type (SFT) consisting of all bi-infinite walks on G_2 is a topological factor of the SFT associated with G_1 given by a 1-block code (see [54] for detailed definitions). Our definition of factor has points of contact with compressed representations of weighted networks, explored in [77], but in general the relationship (4) need not hold for compressed representations.

The definition of factor formalizes the idea that G_2 (the factor) is a collapsed or compressed version of G_1 (the extension). The factor map f associates the vertices in G_2 with a partition of the vertices in G_1 . Condition (4) ensures that the partitioning of the vertices is consistent with the transition probabilities of the random walk on G_1 .

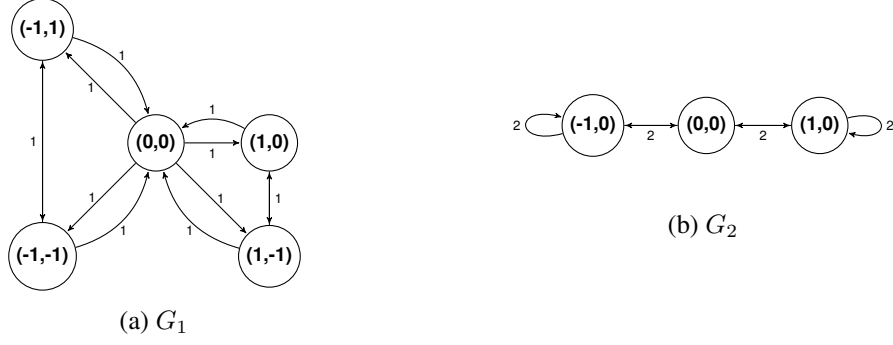


Figure 1: An example of two networks related by a factor map. Here G_2 is a factor of G_1 via the map that collapses vertices along vertical lines.

If P and Q are the transition kernels for G_1 and G_2 , then Condition (4) is equivalent to the statement that for all $v, v' \in V$ and $u \in f^{-1}(v)$,

$$\sum_{u' \in f^{-1}(v')} P(u' | u) = Q(v' | v). \quad (5)$$

This is also equivalent to the condition $\mathbb{P}(f(X_1) = v' | X_0 = u) = \mathbb{P}(Y_1 = v' | Y_0 = v)$, where X and Y are the random walks associated with G_1 and G_2 . Since P and Q are irreducible, Condition (4) implies that the (unique) stationary distributions p on G_1 and q on G_2 are such that for all $v \in V$,

$$\sum_{u \in f^{-1}(v)} p(u) = q(v), \quad (6)$$

which is equivalent to $f(X_1) \stackrel{d}{=} Y_1$. The factor relationship can also be expressed in matrix form. If f is a factor map from G_1 to G_2 , then (4) is equivalent to the condition $PF = FQ$ where $F \in \mathbb{R}^{U \times V}$ is defined by $F(u, v) = 1$ if $f(u) = v$ and $F(u, v) = 0$ otherwise. Furthermore equation (6) is equivalent to $pF = q$.

The next proposition establishes a close connection between transition couplings and factor maps. Let G_1 and G_2 be strongly connected, weighted directed networks with associated random walks X and Y . Note that any stationary Markov coupling (\tilde{X}, \tilde{Y}) of X and Y corresponds to a weighted, directed network H with vertex set $W \subset U \times V$. Let $\pi_U : U \times V \rightarrow U$ and $\pi_V : U \times V \rightarrow V$ be the natural projections onto the first and second coordinates, respectively.

Proposition 13. *If (\tilde{X}, \tilde{Y}) is a stationary Markov coupling corresponding to a strongly connected network H with vertex set W , then (\tilde{X}, \tilde{Y}) is a transition coupling of X and Y if and only if the restriction of π_U to W is a factor map from H to G_1 and the restriction of π_V to W is a factor map from H to G_2 .*

We next investigate connections between factors and deterministic transition couplings.

Definition 14. *Suppose $G_1 = (U, E_1, w_1)$ and $G_2 = (V, E_2, w_2)$ are two strongly connected, weighted, directed networks with associated Markov chains X and Y , respectively. A transition coupling (\tilde{X}, \tilde{Y}) is said to be deterministic from X to Y if for each u in U there exists $v \in V$ such that $\mathbb{P}(\tilde{Y}_0 = v | \tilde{X}_0 = u) = 1$.*

In optimal transport theory, deterministic couplings are associated with the so-called Monge problem, see [82] for more context and discussion. A deterministic coupling (\tilde{X}, \tilde{Y}) from X to Y is associated with a map $f : U \rightarrow V$, where $f(u)$ is the (necessarily unique) element $v \in V$ for which $\mathbb{P}(\tilde{Y}_0 = v | \tilde{X}_0 = u) = 1$. In particular, $(\tilde{X}, \tilde{Y}) \stackrel{d}{=} (X, f(X))$. Moreover, as G_2 is strongly connected, $\mathbb{P}(Y_0 = v) > 0$ for each $v \in V$, and the edge-alignment property (Proposition 2) ensures that f is a surjective graph homomorphism from G_1 to G_2 .

Theorem 15. *Suppose G_1 and G_2 are strongly connected, weighted directed networks with associated random walks X and Y , respectively.*

1. *If G_2 is a factor of G_1 with factor map f , then $Y \stackrel{d}{=} f(X)$, and $(X, f(X))$ is a deterministic transition coupling from X to Y .*
2. *If (\tilde{X}, \tilde{Y}) is a deterministic transition coupling from X to Y , then the induced map $f : U \rightarrow V$ is a factor map from G_1 to G_2 .*

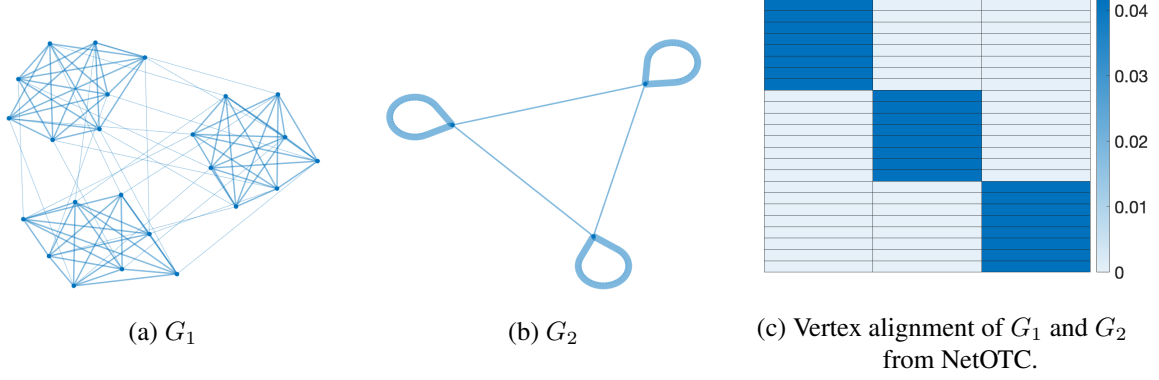


Figure 2: An illustration of the relationship between factors and the NetOTC problem. Under the conditions described in Corollary 17, the NetOTC problem aligns vertices according to the factor map relating the two networks. In this example, G_2 is a factor of G_1 . Figure 2c illustrates the NetOTC vertex alignment, which is supported on pairs of the form $(u, f(u))$.

When G_2 is a factor of G_1 under f , Theorem 15 ensures that $(X, f(X))$ is a transition coupling of their random walks. If the cost function c is such that $c(u, v)$ is minimized by $v = f(u)$ then, as the next result shows, this coupling is also optimal, and there is a deterministic solution to the NetOTC problem.

Definition 16. Let f be a factor map from G_1 to G_2 . A cost function c is compatible with f if $c(u, f(u)) \leq c(u, v)$ for each $u \in U$ and $v \in V$.

One may verify that the cost compatibility condition is satisfied in Example 12 under a Euclidean metric cost.

Corollary 17. Suppose G_1 and G_2 are strongly connected, weighted directed networks and f is a factor map from G_1 to G_2 . If c is compatible with f then $(X, f(X))$ is an OTC of X and Y .

An example illustrating Corollary 17 is given in Figure 2. Corollary 17 provides some insight into the structure of the NetOTC problem. If G_1 and G_2 are related by a factor map $f : U \rightarrow V$, then G_2 is essentially a compressed version of the network G_1 . Corollary 17 ensures that an optimal coupling of the random walks on G_1 and G_2 is obtained by running the random walk on G_1 and mapping every state $u \in U$ in this chain to the corresponding state $f(u) \in V$. In practice, the conclusion of Corollary 17 approximately holds when the factor condition (4) approximately holds; the results of experiments involving exact and approximate factors are given in Section 6.5.

Under the conditions of Corollary 17, the NetOTC cost and associated vertex and edges alignments will have a special form. In particular, the NetOTC cost will satisfy $\rho(G_1, G_2) = \sum_{u \in U} c(u, f(u))p(u)$ where p is the stationary distribution of the random walk on G_1 . Furthermore, $\pi_v(u, v) = \mathbb{I}(f(u) = v)$ and $\pi_e((u, u'), (v, v')) = \mathbb{I}((f(u), f(u')) = (v, v'))$. Note that, while the deterministic coupling appears as a solution of the NetOTC problem, the NetOTC algorithm itself makes no reference to, and does not require prior information about, the factor map f . The next result provides further information about how NetOTC behaves in the presence of factor maps.

Theorem 18. Let G_1, G_2, H_1 , and H_2 be networks with vertex sets U, V, A , and B , and associated Markov chains X, Y, W , and Z , respectively. Suppose that $f : U \rightarrow A$ and $g : V \rightarrow B$ are factor maps from G_1 to H_1 and G_2 to H_2 , and that there are cost functions $c_{ext} : U \times V \rightarrow \mathbb{R}_+$ and $c : A \times B \rightarrow \mathbb{R}_+$ such that $c_{ext}(u, v) = c(f(u), g(v))$.

1. If (\tilde{X}, \tilde{Y}) is an optimal transition coupling of X and Y with respect to c_{ext} , then $(f(\tilde{X}), g(\tilde{Y}))$ is an optimal transition coupling of W and Z with respect to c .
2. If (\tilde{W}, \tilde{Z}) is an optimal transition coupling of W and Z with respect to c , then there exists an optimal transition coupling (\tilde{X}, \tilde{Y}) of X and Y with respect to c_{ext} such that $(f(\tilde{X}), g(\tilde{Y})) \stackrel{d}{=} (\tilde{W}, \tilde{Z})$.

A simple illustration of Theorem 18 is given in Figure 3. For compatible cost functions, the theorem ensures that an optimal transport plan for the extensions G_1 and G_2 can be transferred through the maps f and g to an optimal transport plan for the factors H_1 and H_2 ; moreover, every optimal transport plan for the factors can be

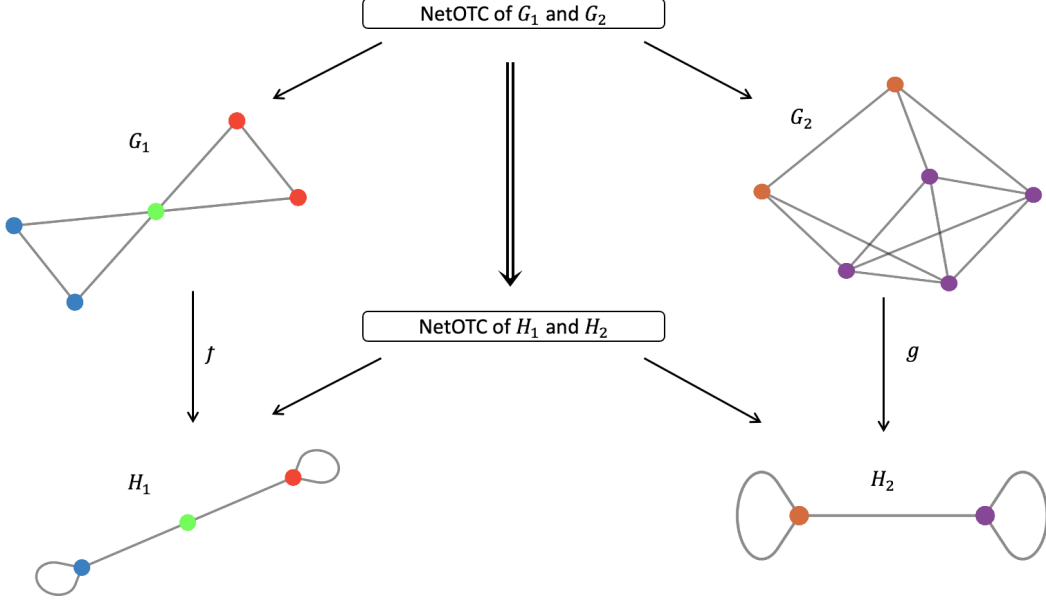


Figure 3: An illustration of Theorem 18. If G_1 and H_1 , and G_2 and H_2 are related by factor maps f and g , respectively, the NetOTC of H_1 and H_2 can be naturally induced by the NetOTC of G_1 and G_2 using the maps f and g .

obtained in this way. Thus NetOTC respects factor structure whenever factor structure is present: the NetOTC alignment of the extensions is consistent with the NetOTC alignment of the factors. This is a fundamental property of the NetOTC procedure, in the sense that the operation of NetOTC on the extensions G_1 and G_2 makes no reference to, and requires no knowledge of, the factor maps f and g or the factors H_1 and H_2 .

6 Example and Experiments

In this section, we illustrate the properties of NetOTC through an example and several numerical experiments. The latter include network classification, network isomorphism, alignment of stochastic block models, and network factors. Complete experimental details may be found in Appendix A. In the example and experiments, we compare NetOTC to several existing, optimal transport-based approaches to network alignment: marginal optimal transport (OT), Gromov-Wasserstein (GW) [68], Fused Gromov-Wasserstein (FGW) [76, 80], and Coordinated Optimal Transport (COPT) [21]. Here marginal optimal transport refers to the optimal coupling of the stationary distributions of the random walks on the given networks. When applying the FGW method, following [76, 80], we use a uniform distribution on the vertices of each network. Code for reproducing the example and experiments may be found at <https://github.com/austinyi/NetOTC>.

6.1 Edge Awareness Example

We begin with a toy example to demonstrate the edge preservation property of NetOTC (see Proposition 2): network G_1 is an octagon network, network G_2 is a copy of G_1 with one edge on the right removed, and network G_3 is topologically identical to G_2 , but its vertices are located in the left half plane. See Figure 4 below.

Table 1 shows the ratio of the costs obtained when comparing different pairs of networks under a cost function equal to the squared Euclidean distance between vertex positions. We considered the methods NetOTC, OT, and FGW, as they allow use of the Euclidean cost function. The ratio of the cost between G_2 and G_1 and the cost between G_2 and G_3 varies greatly between the methods. Observe that NetOTC is the only method with a ratio that exceeds 1, that is, NetOTC finds G_2 to be closer to G_3 than G_1 . This example illustrates that NetOTC is sensitive to topological differences between the given networks, and in particular that topological similarity can dominate differences in the vertex costs.

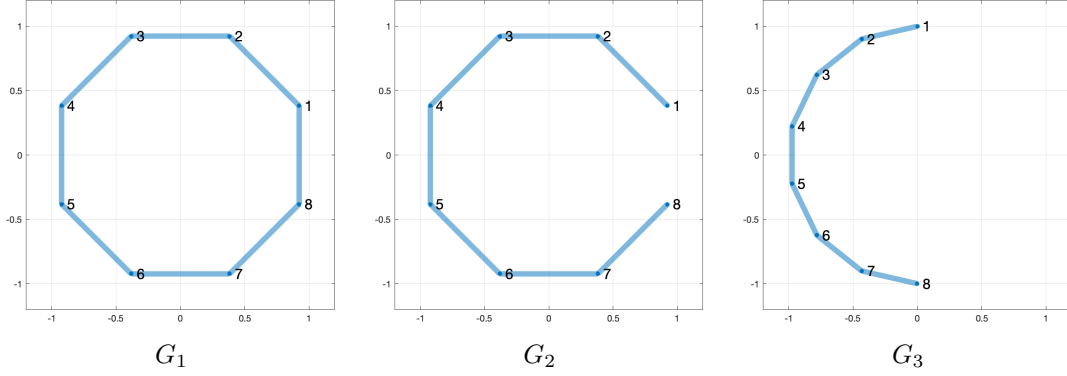


Figure 4: Three networks in which all vertices are located on the unit circle in \mathbb{R}^2 . G_1 is an octagon network. G_2 is obtained by removing an edge G_1 . In G_3 , the vertices are uniformly distributed in the left semicircle.

Algorithm	G_2 vs. G_1	G_2 vs. G_3	Ratio
NetOTC	0.5714	0.4464	1.28
OT	0.2857	0.4464	0.64
FGW	0.0313	0.2725	0.11

Table 1: Comparison of OT-based costs between networks in Figure 4.

6.2 Network Classification

In our next experiment, we examine the utility of NetOTC for network classification tasks. We consider a selection of benchmark network datasets from [43]. Each dataset contains a collection of networks with discrete vertex attributes and class labels. We considered the datasets AIDS [71], BZR [75], Cuneiform [46], MCF-7 [86], MOLT-4 [86], MUTAG [18], and Yeast [86]. For each dataset, we employed an attribute-based cost function, where $c(u, v) = 0$ if vertices u and v have the same attribute and $c(u, v) = 1$ otherwise. For each OT-based comparison method, we constructed a 5-nearest neighbor classifier using a random training set containing 80% of the available networks and used this classifier to predict the labels of the remaining networks.

Table 2 shows the average classification accuracy over 5 random samplings of the training and test sets for each comparison method. As the table demonstrates, NetOTC is competitive with other network OT based methods on the classification tasks, outperforming other methods in several cases, without the need for tuning or specification of free parameters.

Algorithm	AIDS	BZR	Cuneiform	MCF-7	MOLT-4	MUTAG	Yeast
NetOTC	88.0 ± 4.9	84.8 ± 6.6	73.2 ± 7.8	92.8 ± 4.2	92.0 ± 2.0	85.4 ± 7.1	90.8 ± 6.4
OT	84.4 ± 6.1	76.4 ± 4.6	71.3 ± 7.7	93.6 ± 3.3	92.0 ± 2.0	63.2 ± 7.3	91.2 ± 7.0
GW	98.8 ± 1.8	78.0 ± 8.5	12.8 ± 4.6	93.6 ± 3.3	91.6 ± 2.6	81.6 ± 7.0	91.6 ± 6.2
FGW	99.2 ± 1.1	80.0 ± 7.1	74.8 ± 3.6	92.8 ± 4.2	91.6 ± 2.6	84.3 ± 8.6	89.2 ± 6.6
COPT	98.0 ± 1.4	73.6 ± 7.9	16.6 ± 3.1	92.4 ± 4.8	91.6 ± 2.6	80.0 ± 5.6	90.4 ± 6.7

Table 2: 5-nearest neighbor classification accuracies for networks with discrete vertex attributes. Average accuracies observed over 5 random samplings of the training and test sets are reported along with their standard deviation.

6.3 Network Isomorphism

Two undirected, unweighted networks $G_1 = (U, E_1)$ and $G_2 = (V, E_2)$ are isomorphic if there is a bijection $\phi : U \rightarrow V$ of their vertex sets that preserves edges in the sense that $(u, u') \in E_1$ if and only if $(\phi(u), \phi(u')) \in E_2$. Determining when two networks are isomorphic, and if so identifying an isomorphism, are important problems in network theory that have received much attention in the literature [59, 12]. In general, it is challenging to find isomorphisms in an efficient fashion [4].

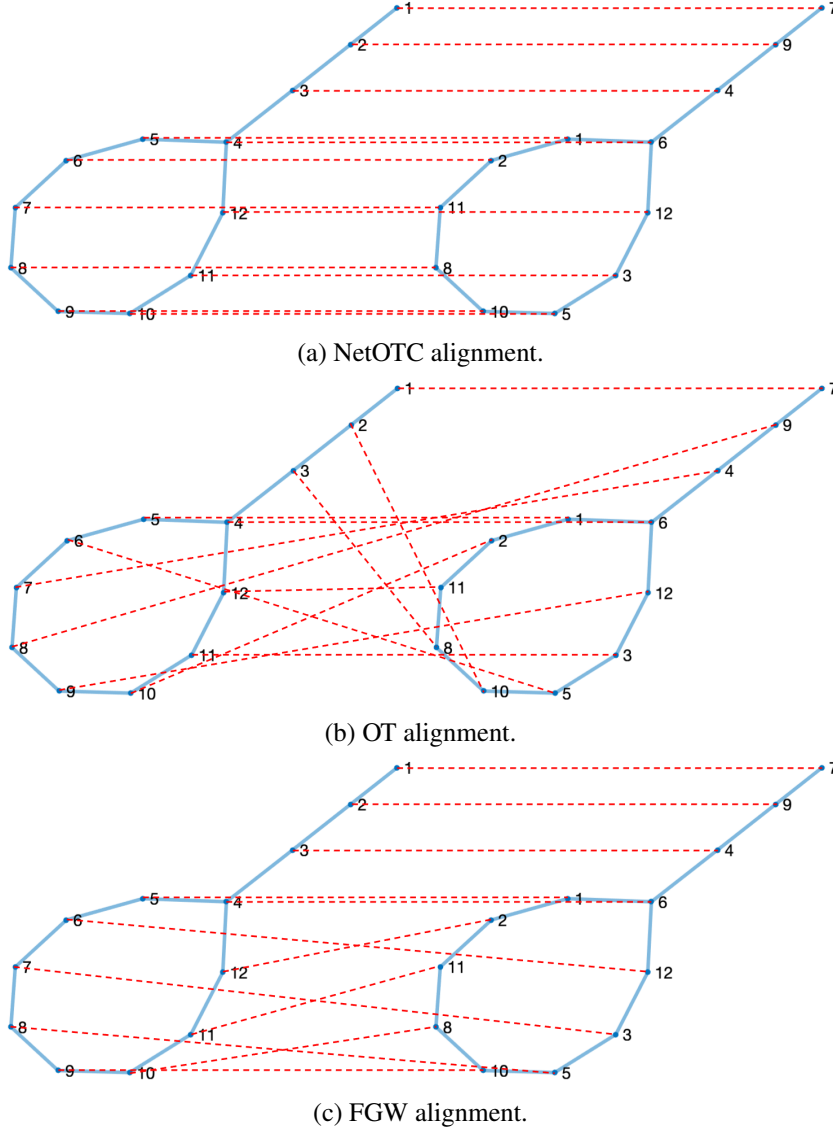


Figure 5: Alignment of two isomorphic lollipop networks obtained by NetOTC, OT and FGW. NetOTC correctly detects the vertex isomorphism map, while other methods cannot.

To evaluate the ability of the alignment methods under study to successfully identify network isomorphisms, we carried out the following experiment. Given a network G_1 , we create an isomorphic copy G_2 by applying a permutation ϕ to its vertices. We then applied NetOTC, FGW, GW, and OT to G_1 and G_2 with a degree-based cost function. From each method we obtained a soft vertex alignment $\pi_v : U \times V \rightarrow \mathbb{R}_+$ of the given networks, and from π_v we derived a hard vertex alignment $\psi(u) = \operatorname{argmax}_{v \in V} \pi_v(u, v)$. If the hard alignment ψ is identical to the isomorphism ϕ , the algorithm has successfully identified the isomorphism. See Appendix A.2 for more details. Figure 5 shows an example of isomorphic “lollipop” networks (a similar example is shown in Appendix A.2 Figure 8). NetOTC correctly detects the isomorphism, but the other methods do not. Note that the cost function used by each method to align the vertices depends only on their degree, and that the majority of the vertices in the lollipop network have degree 2. This suggests that the edge awareness of NetOTC (see Proposition 2) plays an important role in recovering the isomorphism.

Further experiments demonstrate the ability of NetOTC to recover isomorphisms in different classes of networks: random (Erdos-Renyi) networks, stochastic block models (SBMs), networks with a random weighted (0,1,2) adjacency matrix, and random lollipop networks. Table 3 shows the average performance of each method for 300 random networks of each class. See Appendix A.2 for further details of the network generation process. NetOTC exhibits perfect performance for networks with random adjacency matrices and all types of SBMs, with very high accuracy in Erdos-Renyi and random lollipop networks. On all classes but random adjacency matrix, the competing methods perform markedly worse. The poor performance of OT demonstrates the substantial

	NetOTC	FGW	GW	OT
Erdos-Renyi ($n \in \{6, \dots, 15\}, p = 1/3$)	96.73	71.50	54.67	2.80
Erdos-Renyi ($n \in \{6, \dots, 15\}, p = 2/3$)	94.86	57.19	48.63	8.56
Erdos-Renyi ($n \in \{16, \dots, 25\}, p = 1/4$)	99.64	88.45	69.68	0.00
Erdos-Renyi ($n \in \{16, \dots, 25\}, p = 3/4$)	100.00	71.33	50.00	0.00
SBM (7, 7, 7, 7)	100.00	84.62	54.85	0.00
SBM (10, 8, 6)	100.00	78.33	58.67	0.00
SBM (7, 7, 7)	100.00	71.28	41.89	0.00
Random weighted adjacency matrix $\{0, 1, 2\}$	100.00	96.67	96.33	5.67
Random Lollipop network	98.00	13.67	6.00	0.00

Table 3: Isomorphism detection success rate (%). We generate 300 random networks in each class. For each random network, we also permute its vertices and apply the algorithms to the two isomorphic networks. We report the percentage of times the output alignment of each algorithm is an isomorphism.

performance gains obtained from coupling the full random walks on G_1 and G_2 , rather than their stationary distributions.

6.4 Block Alignment in Stochastic Block Models

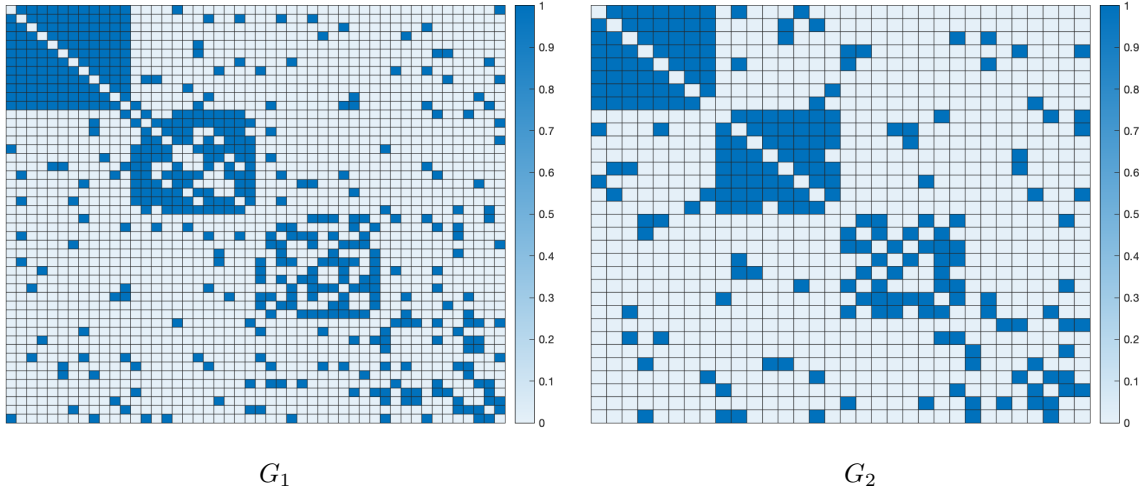


Figure 6: The adjacency matrices of random networks G_1 and G_2 drawn from SBMs. We can easily check the block structure due to different connection probabilities within the block. G_1 and G_2 are designed to have the same block structure with a different number of vertices.

Stochastic block models [36] (SBMs) are frequently used to model random networks with community structure. SBMs have found application in a variety of network problems, including community detection and network clustering, see for example [1, 49, 2]. In an SBM, each vertex is assigned (deterministically or at random) to one of a small number of groups, also known as blocks. Once group assignment is complete, edges are placed between pairs of vertices independently, with the probability of an edge being present depending on the group assignments of its endpoints. In most cases, edge probabilities are higher within groups than between groups, so that the vertices in a group constitute, informally at least, a community.

We wished to assess the ability of OT-based comparison methods to align the vertices and edges of stochastically equivalent blocks in SBMs of different sizes. To this end, we generated 10 realizations G_1, G_2 of SBMs with 4 blocks. In each case, the network G_1 had 12 vertices per block, and G_2 had 8 vertices per block. For each network, the within block connection probabilities were 1, 0.8, 0.6, and 0.4, while the between block connection probability was equal to 0.1. The adjacency matrix of a typical realization of G_1 and G_2 is depicted in Figure 6. Note that the networks G_1 and G_2 are undirected and unweighted.

We applied the five comparison methods under study to each of the 10 realizations of G_1 and G_2 using the

standardized degree-based cost function. Each method returns a vertex alignment $\pi_v : U \times V \rightarrow \mathbb{R}_+$ associated with the respective optimal transport plans. Vertex alignment accuracy was assessed by summing π_v over vertex pairs in corresponding blocks, i.e., blocks with the same connection probability.

As described above, the NetOTC optimal transport plan also provides a native edge alignment $\pi_e : U^2 \times V^2 \rightarrow \mathbb{R}_+$. For other methods, we formed an edge alignment by setting $\pi_e((u, u'), (v, v')) = \pi_v(u, v)\pi_v(u', v')$. Edge alignment accuracy was evaluated by summing the alignment probabilities of all pairs of edges connecting stochastically equivalent blocks, i.e., summing all $\pi_e((u, u'), (v, v'))$ where u and v , and u' and v' are from blocks with equal connection probabilities.

Figure 7 shows the vertex and edge alignment accuracies for each of the methods tested. As background, we note that random guessing yields an accuracy of 25% for vertex alignment and 6.25% for edge alignment. For vertex alignment, NetOTC, GW, and FGW exhibit similar performance (substantially better than random guessing) while OT and COPT do worse. As indicated by the error bars in Figure 7, the vertex alignment accuracy of NetOTC has substantially lower variance than the accuracies of OT, GW, and FGW. As expected, NetOTC outperforms other methods from the standpoint of edge alignment.

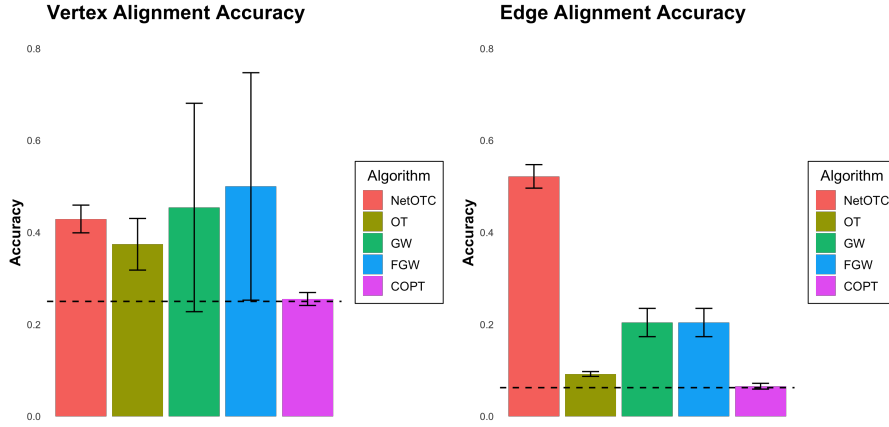


Figure 7: SBM alignment accuracies. Average accuracies observed over 10 random pairs of SBMs are reported along with their standard deviation. The horizontal dashed line in each plot indicates the accuracy of random guessing.

6.5 Network Factors

Lastly, we considered the task of aligning corresponding vertices when the network G_2 is a factor of G_1 and the cost is compatible with the factor map (see Section 5.4). We construct networks G_1 and G_2 via vertex embeddings in \mathbb{R}^5 as follows. The network G_2 has 6 vertices, each associated with a feature vector generated from a 5-dimensional normal distribution with mean zero and variance $\sigma^2 \mathbf{I}$. The network G_1 has 30 vertices, each associated with a feature vector sampled from a 6-component Gaussian mixture model. The means of the 6 components correspond to the feature vectors associated with the 6 vertices of G_2 , while the variances are \mathbf{I}_5 . Here, the factor map f is determined by the component from which the feature vector was sampled. Next, we randomly set the edge weights of network G_2 to an integer between 1 and 10. Then, the edge weights of network G_1 are randomly determined so that equation (4) holds, and therefore G_2 is a factor of G_1 . The networks considered are undirected, in order to enable comparison with other methods. See Table 5 of Appendix A.4 for results on directed networks; there was no significant difference in the performance of NetOTC between directed and undirected networks. The experiment was repeated in a setting where G_2 is an approximate factor of G_1 , that is, when the factor condition only holds approximately. See Appendix A.4 for explanations of how we generated an approximate factor.

NetOTC, FGW, and OT were applied to the generated networks G_1 and G_2 using an embedding-based cost equal to the squared Euclidean distances between the vectors associated with the vertices. Table 4 reports the vertex alignment accuracy of each method for different values of the variance σ^2 . Vertex alignment accuracy was assessed by summing the mass of the optimal coupling on factor pairs of the form $(u, f(u))$. NetOTC outperforms the other methods, with the performance gap growing as σ decreases. For an exact factor with compatible cost, which occurs when $\sigma = 2.5$, NetOTC returns a perfect alignment, as guaranteed by Corollary 17. Results from other cases demonstrate that the performance of NetOTC is robust when the factor and cost conditions hold only

approximately. It is also noteworthy that FGW and OT yield nearly identical alignment accuracy in all cases.

	Exact factor			Approximate factor		
	NetOTC	FGW	OT	NetOTC	FGW	OT
$\sigma = 2.5$	100.00 \pm 0.00	98.17 \pm 3.95	98.38 \pm 3.40	98.57 \pm 0.20	98.07 \pm 4.55	98.32 \pm 3.96
$\sigma = 2.0$	99.95 \pm 0.46	96.57 \pm 5.22	96.75 \pm 5.08	98.09 \pm 1.64	95.83 \pm 5.35	96.00 \pm 5.11
$\sigma = 1.5$	97.45 \pm 5.10	90.20 \pm 8.24	90.57 \pm 8.18	96.43 \pm 4.40	91.23 \pm 7.85	91.65 \pm 7.72
$\sigma = 1.0$	81.60 \pm 13.88	73.23 \pm 12.08	73.85 \pm 12.05	79.44 \pm 12.14	72.00 \pm 11.74	72.00 \pm 12.06

Table 4: Undirected networks: alignment accuracies of network factors. Average accuracies observed over 100 random network factors are reported along with their standard deviation.

7 Proofs

In this section, we provide the proofs of our results. Before proceeding, we introduce some necessary background. Given two stationary processes $X = X_0, X_1, \dots$ and $Y = Y_0, Y_1, \dots$ taking values in finite sets U and V , respectively, and a cost $c : U \times V \rightarrow \mathbb{R}_+$, the optimal joining distance $\mathcal{S}_c(X, Y)$ is the minimum of $\mathbb{E}[c(\tilde{X}_0, \tilde{Y}_0)]$ over stationary couplings (\tilde{X}, \tilde{Y}) of X and Y . Stationary couplings are referred to as *joinings* in the ergodic theory literature [29, 17]. As every transition coupling of stationary Markov chains X and Y is also a joining, we have

$$\mathcal{S}_c(X, Y) \leq \min_{(\tilde{X}, \tilde{Y}) \in \Pi_{TC}(X, Y)} \mathbb{E}c(\tilde{X}_0, \tilde{Y}_0) = \rho(G_1, G_2) \quad (7)$$

When c is a metric, $\mathcal{S}_c(\cdot, \cdot)$ is a metric between stationary processes [33].

Now we introduce some additional notation. For any finite set S , let Δ_S denote the set of probability distributions on S . We will regard $\lambda \in \Delta_S$ as a row vector, and write $\lambda(s)$ for the λ -probability of $s \in S$. If $g : S \rightarrow \mathbb{R}$ is any function, let $\langle \lambda, g \rangle = \sum_{s \in S} \lambda(s)g(s)$, which is the expectation of g with respect to λ . For stochastic matrices (equivalently, Markov transition kernels) P and Q let $\Pi_{TC}(P, Q)$ denote the set of stochastic matrices R satisfying the transition coupling condition (1). By Proposition 4 in [64] the NetOTC cost can be written as $\rho(G_1, G_2) = \min \{ \langle \lambda, c \rangle : R \in \Pi_{TC}(P, Q), \lambda R = \lambda, \lambda \in \Delta_{U \times V} \}$.

7.1 Result for NetOTC Edge Preservation

Proposition 2. *Let π_e be the NetOTC edge alignment of networks $G_1 = (U, E_1, w_1)$ and $G_2 = (V, E_2, w_2)$ based on the optimal transport plan (X^*, Y^*) . If $\pi_e((u, u'), (v, v')) > 0$ then $(u, u') \in E_1$ and $(v, v') \in E_2$.*

Proof. Let P and Q be the transition kernels associated with graphs G_1 and G_2 , and let

$$\lambda^*, R^* = \operatorname{argmin}_{\lambda, R} \{ \langle \lambda, c \rangle : R \in \Pi_{TC}(P, Q), \lambda R = \lambda, \lambda \in \Delta_{|U| \times |V|} \},$$

be a solution for the NetOTC problem. The edge alignment probability can be expressed in terms of λ^*, R^* as $\pi_e((u, u'), (v, v')) = \lambda^*(u, v) R^*(u', v' | u, v)$. Since $R^* \in \Pi_{TC}(P, Q)$ and $\pi_e((u, u'), (v, v')) > 0$, we have

$$\begin{aligned} P(u' | u) &= \sum_{\tilde{v} \in V} R^*(u', \tilde{v} | u, v) \geq R^*(u', v' | u, v) > 0, \\ Q(v' | v) &= \sum_{\tilde{u} \in U} R^*(\tilde{u}, v' | u, v) \geq R^*(u', v' | u, v) > 0, \end{aligned}$$

which implies $(u, u') \in E_1$ and $(v, v') \in E_2$. □

7.2 Properties of $\rho(G_1, G_2)$

Proposition 4. *Let G_1 and G_2 be networks with associated random walks X and Y . Then*

$$\rho(G_1, G_2) = \min_{(\tilde{X}, \tilde{Y}) \in \Pi_{TC}(X, Y)} \mathbb{E}\tilde{c}(\tilde{X}, \tilde{Y}),$$

and the optimal transport plans minimizing $\mathbb{E}\tilde{c}(\tilde{X}, \tilde{Y})$ coincide with those minimizing $\mathbb{E}c(\tilde{X}_0, \tilde{Y}_0)$.

Proof. Let (\tilde{X}, \tilde{Y}) be a transition coupling of X and Y . As (\tilde{X}, \tilde{Y}) is stationary, the ergodic theorem ensures that the limit

$$\hat{c}(\tilde{X}, \tilde{Y}) := \lim_k c_k(\tilde{X}_0^{k-1}, \tilde{Y}_0^{k-1})$$

exists almost surely and that $\mathbb{E}\hat{c}(\tilde{X}, \tilde{Y}) = \mathbb{E}c(\tilde{X}, \tilde{Y})$. It then follows from the definition of \bar{c} that

$$\mathbb{E}\bar{c}(\tilde{X}, \tilde{Y}) = \mathbb{E}\hat{c}(\tilde{X}, \tilde{Y}) = \mathbb{E}c(\tilde{X}, \tilde{Y}).$$

Taking minima over the set of all transition couplings of X and Y yields the result. \square

Proposition 5. *Let G_1 and G_2 be networks with associated random walks X and Y . For each $k \geq 1$*

$$\rho(G_1, G_2) \geq \min \mathbb{E} c_k(\tilde{X}_0^{k-1}, \tilde{Y}_0^{k-1}),$$

where the minimum is over the family of all couplings of X_0^{k-1} and Y_0^{k-1} .

Proof. Every transition coupling of X and Y is also a joining of X and Y and therefore, as noted in (7), $\rho(G_1, G_2) \geq \mathcal{S}_c(X, Y)$. Let (\tilde{X}, \tilde{Y}) be any joining of X and Y . Stationarity of (\tilde{X}, \tilde{Y}) implies that

$$\mathbb{E}c(\tilde{X}_0, \tilde{Y}_0) = \mathbb{E}c_k(\tilde{X}_0^{k-1}, \tilde{Y}_0^{k-1})$$

and therefore $\mathcal{S}_c(X, Y) = \mathcal{S}_{c_k}(X, Y)$. Moreover, $(\tilde{X}_0^{k-1}, \tilde{Y}_0^{k-1})$ is also a coupling of X_0^{k-1} and Y_1^k so

$$\mathcal{S}_{c_k}(X, Y) \geq \min_{(\tilde{X}_0^{k-1}, \tilde{Y}_0^{k-1}) \in \Pi(X_0^{k-1}, Y_0^{k-1})} \mathbb{E}c_k(\tilde{X}_0^{k-1}, \tilde{Y}_0^{k-1}).$$

Combining these inequalities gives the result. \square

7.3 Results for Undirected Networks with a Common Vertex Set

Here we consider undirected networks on a common vertex set. We assume that the networks are connected. Throughout this section, we will make use of the well-known fact that the stationary distribution of a simple random walk $X = X_0, X_1, \dots$ on a connected undirected network $G = (U, E, w)$ satisfies $p(u) = d(u)/D$, where $d(u)$ is the weighted degree of u and D is the sum of all the weights in the network.

Proposition 7. *Connected undirected networks G_1 and G_2 are equivalent if and only if their respective random walks are identical.*

Proof. Let $d_1(u) = \sum_{u' \in U} w_1(u, u')$ and $d_2(u) = \sum_{u' \in U} w_2(u, u')$ be the degree functions for G_1 and G_2 . Suppose first that $G_1 \sim G_2$ and thus there exists $C > 0$ such that $w_1(u, u') = Cw_2(u, u')$ for every $u, u' \in U$. Then the two transition matrices P and Q associated with G_1 and G_2 are equal since

$$P(u'|u) = \frac{w_1(u, u')}{d_1(u)} = \frac{w_2(u, u')}{d_2(u)} = Q(u'|u).$$

Suppose now that P and Q are equal. Then for every $(u, u') \in E_1$, we have

$$\frac{w_1(u, u')}{d_1(u)} = \frac{w_2(u, u')}{d_2(u)},$$

or equivalently $w_1(u, u') = C_u w_2(u, u')$ where $C_u = d_1(u)/d_2(u)$. As G_1 and G_2 are undirected, it is easy to see that $C_u = C_{u'}$. As G_1 and G_2 are connected, there exists a sequence of edges $(u_1, u_2), (u_2, u_3), \dots, (u_{n-1}, u_n) \in E$ such that $U \subseteq \{u_1, \dots, u_n\}$. Repeating the arguments above for all edges in this sequence we conclude that $C_u = C_{u'}$ for every $u, u' \in U$, and it follows that $G_1 \sim G_2$. \square

Proposition 8. *If the cost function $c : U \times U \rightarrow \mathbb{R}_+$ satisfies the properties of a metric on U , then ρ is a metric on the equivalence classes of undirected networks with vertex set contained in U defined by \sim .*

Proof. The symmetry of ρ is clear. It is established in Proposition 25 of [64] that the optimal transition coupling cost satisfies the triangle inequality for Markov chains when the cost c does, and therefore ρ satisfies the triangle inequality. Thus it suffices to show that $\rho(G_1, G_2) = 0$ if and only if $G_1 \sim G_2$. Let G_1 and G_2 be networks satisfying $G_1 \sim G_2$ with associated transition matrices P and Q . By Proposition 7, P and Q are equal and clearly

$\rho(G_1, G_2) = 0$ since $\langle \lambda, c \rangle = 0$ is achieved by λ satisfying $\lambda(u, v) = p(u)\mathbb{I}(u = v)$, which is stationary for the transition coupling satisfying

$$R(u', v'|u, v) = \begin{cases} P(u'|u)\mathbb{I}(u' = v') & u = v \\ P(u'|u)P(v'|v) & \text{otherwise} \end{cases}.$$

Now suppose that $G_1 \approx G_2$. By Proposition 7, P and Q are necessarily distinct, and consequently so are their associated stationary Markov chains. As it defines a distance on stationary processes $\mathcal{S}_c(X, Y) > 0$, and applying (7), we conclude that $\rho(G_1, G_2) > 0$ as well. \square

Proposition 10. *Let G_1 and G_2 be undirected networks with the same vertex set. Let $d_1(u)$ and $d_2(u)$ be the degree functions of G_1 and G_2 , respectively, and assume that each network has total degree D . Then under the zero-one cost $c(u, u') = \mathbb{I}(u \neq u')$,*

- $\rho(G_1, G_2) \geq \frac{1}{2D} \sum_{u \in U} |d_1(u) - d_2(u)|$
- $\rho(G_1, G_2) \geq \frac{1}{4D} \sum_{u, u' \in U} |w_1(u, u') - w_2(u, u')|$

Proof. The random walks X and Y associated with G_1 and G_2 have stationary distributions $p(u) = d_1(u)/D$ and $q(u) = d_2(u)/D$. Using the well-known connection between total variation distance and optimal transport with under the 0-1 cost (see, e.g., [82]), we have

$$\begin{aligned} \min_{(\tilde{X}_0, \tilde{Y}_0) \in \Pi(X_0, Y_0)} \mathbb{E}c(\tilde{X}_0, \tilde{Y}_0) &= \min_{(\tilde{X}_0, \tilde{Y}_0) \in \Pi(X_0, Y_0)} \mathbb{E}\mathbb{I}(\tilde{X}_0, \tilde{Y}_0) \\ &= \frac{1}{2} \sum_{u \in U} |p(u) - q(u)| = \frac{1}{2D} \sum_{u \in U} |d_1(u) - d_2(u)|. \end{aligned}$$

Applying Proposition 5 yields the bound for $k = 1$. To obtain the bound for $k = 2$, let $\delta_2((u, u'), (v, v')) = \mathbb{I}((u, u') \neq (v, v'))$ and note that

$$\delta_2((u, u'), (v, v')) \leq \mathbb{I}(u \neq v) + \mathbb{I}(u' \neq v') = 2c_2((u, v), (u', v')).$$

By Proposition 5,

$$\rho(G_1, G_2) \geq \min_{(\tilde{X}_0^1, \tilde{Y}_0^1) \in \Pi(X_0^1, Y_0^1)} \mathbb{E}c_2(\tilde{X}_0^1, \tilde{Y}_0^1) \geq \frac{1}{2} \min_{(\tilde{X}_0^1, \tilde{Y}_0^1) \in \Pi(X_0^1, Y_0^1)} \mathbb{E}\delta_2(\tilde{X}_0^1, \tilde{Y}_0^1).$$

Then using the connection between the transport cost with respect to δ_2 and the total variation distance once again, we obtain

$$\begin{aligned} \rho(G_1, G_2) &\geq \frac{1}{4} \sum_{u, u' \in U} |\mathbb{P}(X_0^1 = (u, u')) - \mathbb{P}(Y_0^1 = (u, u'))| \\ &= \frac{1}{4} \sum_{u, u' \in U} |p(u)\mathbb{P}(X_1 = u' | X_0 = u) - q(u)\mathbb{P}(Y_1 = u' | Y_0 = u)| \\ &= \frac{1}{4} \sum_{u, u' \in U} \left| \frac{d_1(u)}{D} \frac{w_1(u, u')}{d_1(u)} - \frac{d_2(u)}{D} \frac{w_2(u, u')}{d_2(u)} \right| \\ &= \frac{1}{4D} \sum_{u, u' \in U} |w_1(u, u') - w_2(u, u')|. \end{aligned}$$

\square

7.4 Results Concerning Network Factors

In this section, we prove the results about factor maps, including Theorems 15 and 18.

Proposition 13. *If (\tilde{X}, \tilde{Y}) is a stationary Markov coupling corresponding to a strongly connected network H with vertex set W , then (\tilde{X}, \tilde{Y}) is a transition coupling of X and Y if and only if the restriction of π_U to W is a factor map from H to G_1 and the restriction of π_V to W is a factor map from H to G_2 .*

Proof. In this setting, the conditions in Definition 1 for (\tilde{X}, \tilde{Y}) to be a transition coupling are precisely equivalent to Condition 4 for the restrictions of π_U and π_V to W . \square

Theorem 15. Suppose G_1 and G_2 are strongly connected, weighted directed networks with associated random walks X and Y , respectively.

1. If G_2 is a factor of G_1 with factor map f , then $Y \stackrel{d}{=} f(X)$, and $(X, f(X))$ is a deterministic transition coupling from X to Y .
2. If (\tilde{X}, \tilde{Y}) is a deterministic transition coupling from X to Y , then the induced map $f : U \rightarrow V$ is a factor map from G_1 to G_2 .

Proof. To prove 1., let f be a factor map from G_1 to G_2 . We first show $Y \stackrel{d}{=} f(X)$. In order to simplify notation, we will let $f(X_0^{n-1}) = f(X_0), \dots, f(X_{n-1})$. Let us prove by induction that for any $v_0^n \in V$, we have

$$\mathbb{P}(f(X_0^n) = v_0^n) = \mathbb{P}(Y_0^n = v_0^n).$$

The base case ($n = 0$) is immediate from Equation (6). For the inductive step, we suppose it is true for some $n \geq 0$. Let $v_0^{n+1} \in V$. Then we have

$$\begin{aligned} \mathbb{P}(f(X_0^n) = v_0^{n+1}) &= \sum_{u_0^{n+1} \in f^{-1}(v_0^{n+1})} \mathbb{P}(X_0^{n+1} = u_0^{n+1}) \\ &= \sum_{u_0^{n+1} \in f^{-1}(v_0^{n+1})} \mathbb{P}(X_0^n = u_0^n) \cdot \mathbb{P}(X_{n+1} = u_{n+1} \mid X_0^n = u_0^n) \\ &= \sum_{u_0^n \in f^{-1}(v_0^n)} \mathbb{P}(X_0^n = u_0^n) \cdot \sum_{u_{n+1} \in f^{-1}(v_{n+1})} \mathbb{P}(u_{n+1} \mid u_n) \\ &= Q(v_{n+1} \mid v_n) \cdot \sum_{u_0^n \in f^{-1}(v_0^n)} \mathbb{P}(X_0^n = u_0^n) \\ &= \mathbb{P}(Y_{n+1} = v_{n+1} \mid Y_n = v_n) \cdot \mathbb{P}(Y_0^n = v_0^n) \\ &= \mathbb{P}(Y_0^{n+1} = v_0^{n+1}), \end{aligned}$$

where we have used Equation (5) and the inductive hypothesis.

Next, we show that $(X, f(X))$ is a transition coupling of X and Y . We begin by verifying that $(X, f(X))$ is Markov. Fixing $(u, v) \in U \times V$ and $n \geq 1$, we have

$$\begin{aligned} \mathbb{P}((X_n, f(X_n)) = (u, v) \mid \{(X_i, f(X_i))\}_{i < n}) &= \mathbb{P}((X_n, f(X_n)) = (u, v) \mid \{X_i\}_{i < n}) \\ &= \mathbb{P}(X_n = u \mid \{X_i\}_{i < n}) \mathbb{I}(f(u) = v) \\ &= \mathbb{P}(X_n = u \mid X_{n-1}) \mathbb{I}(f(u) = v) \\ &= \mathbb{P}((X_n, f(X_n)) = (u, v) \mid X_{n-1}) \\ &= \mathbb{P}((X_n, f(X_n)) = (u, v) \mid (X_{n-1}, f(X_{n-1}))), \end{aligned}$$

so the process $(X, f(X))$ is Markov.

This Markov chain clearly has a U marginal that is equal in distribution to X and the V marginal is equal in distribution to Y as we proved above. Thus the joint process is a coupling of X and Y . So it suffices to check the transition coupling condition. Let $R \in [0, 1]^{|U||V| \times |U||V|}$ denote the transition matrix satisfying

$$R(u', v' \mid u, v) = \begin{cases} \mathbb{P}(u' \mid u) \mathbb{I}(f(u') = v') & f(u) = v \\ \mathbb{P}(u' \mid u) Q(v' \mid v) & \text{otherwise} \end{cases}.$$

Let p be the stationary distribution of X . Then $\lambda(u, v) = p(u) \mathbb{I}(f(u) = v)$ is equal in distribution to

$(X_0, f(X_0))$. Observe that for all $(u', v') \in U \times V$, we have

$$\begin{aligned}
\sum_{(u,v) \in U \times V} \lambda(u, v) R(u', v' | u, v) &= \sum_{(u,v) \in U \times V} p(u) \mathbb{I}(f(u) = v) P(u' | u) \mathbb{I}(f(u') = v') \\
&= \mathbb{I}(f(u') = v') \sum_{v \in V} \sum_{u \in f^{-1}(v)} p(u) P(u' | u) \\
&= \mathbb{I}(f(u') = v') \sum_{u \in U} p(u) P(u' | u) \\
&= p(u') \mathbb{I}(f(u') = v') \\
&= \lambda(u', v'),
\end{aligned}$$

and therefore λ is stationary for R . So lastly, we only need to show that $R \in \Pi_{TC}(P, Q)$. For pairs $(u, v) \in U \times V$ with $f(u) \neq v$, we see that $R(\cdot | u, v)$ is the independent coupling of $P(\cdot | u)$ and $Q(\cdot | v)$, which clearly satisfies the transition coupling condition. Thus we need only check the transition coupling condition for pairs (u, v) satisfying $f(u) = v$. Let $u, u' \in U$ and $v \in V$ and suppose that $f(u) = v$. Then

$$\sum_{v' \in V} R(u', v' | u, v) = \sum_{v' \in V} P(u' | u) \mathbb{I}(f(u') = v') = P(u' | u).$$

Now checking the other half of the transition coupling condition, let $u \in U$ and $v, v' \in V$ be such that $f(u) = v$. Then by Equation (5), we have

$$\sum_{u' \in U} R(u', v' | u, v) = \sum_{u' \in U} P(u' | u) \mathbb{I}(f(u') = v') = \sum_{u' \in f^{-1}(v')} P(u' | u) = Q(v' | v).$$

Thus $(X, f(X))$ is a transition coupling of X and Y . It is forward-deterministic by construction.

Now we prove 2. To that end, suppose (\tilde{X}, \tilde{Y}) is a forward-deterministic coupling of X and Y , and let $f : U \rightarrow V$ be the induced map. For notation, let R be the transition matrix associated to the joint Markov chain (\tilde{X}, \tilde{Y}) . To verify that f is a factor map, let $v, v' \in V$ and $u \in f^{-1}(v)$. Since (\tilde{X}, \tilde{Y}) is forward deterministic, for every $u' \in f^{-1}(v')$ we have that $P(u' | u) = R((u', v') | (u, v))$. Then, also using the transition coupling property of R , we see that

$$\sum_{u' \in f^{-1}(v')} P(u' | u) = \sum_{u' \in f^{-1}(v')} R((u', v') | (u, v)) = \sum_{u' \in U} R((u', v') | (u, v)) = Q(v' | v).$$

□

Corollary 17. Suppose G_1 and G_2 are strongly connected, weighted directed networks and f is a factor map from G_1 to G_2 . If c is compatible with f then $(X, f(X))$ is an OTC of X and Y .

Proof. By part 1. of Theorem 15, we have that $(X, f(X))$ is a transition coupling of X and Y . Let (\tilde{X}, \tilde{Y}) be any transition coupling of X and Y . Then,

$$\mathbb{E}c(\tilde{X}_0, \tilde{Y}_0) \geq \mathbb{E}c(\tilde{X}_0, f(\tilde{X}_0)) = \mathbb{E}c(X_0, f(X_0)).$$

Taking an infimum over all transition couplings (\tilde{X}, \tilde{Y}) of X and Y , we conclude that $(X, f(X))$ is an optimal transition coupling of X and Y , as desired. □

In the following proof of our two-factor result (Theorem 18), we will use the notion of relatively independent couplings. Suppose X , Y , and Z are random variables and there are maps f and g such that $f(X) \stackrel{d}{=} Z$ and $g(Y) \stackrel{d}{=} Z$. The main property that we need is that there exists a coupling (\tilde{X}, \tilde{Y}) of X and Y such that $f(\tilde{X}) = g(\tilde{Y})$ almost surely. The existence of such a coupling is usually demonstrated by constructing the *relatively independent coupling* of X and Y over Z , which is defined by the property that

$$\mathbb{P}(\tilde{X} \in A, \tilde{Y} \in B) = \mathbb{E}[\mathbb{P}(X \in A | Z) \cdot \mathbb{P}(Y \in B | Z)],$$

where the expectation is taken with respect to Z . In words, the relatively independent coupling makes \tilde{X} and \tilde{Y} conditionally independent given Z . This construction is useful in optimal transport for proving the triangle inequality. In the context of ergodic theory, when the random variables are replaced by stationary processes, it is called the relatively independent joining of X and Y [16]. We note if the stationary processes are the random walks on some strongly connected networks and the maps f and g are factor maps in the sense of Section 5.4, then the relatively independent joinings are in fact transition couplings.

Proposition 19. Suppose $G_1 = (U, E_1, w_1)$, $G_2 = (V, E_2, w_2)$, and $G_3 = (W, E_3, w_3)$ are strongly connected weighted directed networks with associated random walks X , Y , and Z . Further suppose that there are factor maps $f : U \rightarrow W$ from G_1 to G_3 and $g : V \rightarrow W$ from G_2 to G_3 . Then there is a transition coupling (\tilde{X}, \tilde{Y}) of X and Y such that $f(\tilde{X}) = g(\tilde{Y})$ holds almost surely.

Proof. Define the coupling (\tilde{X}, \tilde{Y}) to be the Markov chain with stationary distribution r and transition kernel R given as follows. For $w \in W$ with $\mathbb{P}(Z_0 = w) > 0$ and $(u, v) \in U \times V$ such that $f(u) = g(v) = w$, let

$$r(u, v) = \frac{p(u) \cdot q(v)}{\mathbb{P}(Z_0 = w)},$$

and otherwise let $r(u, v) = 0$. Furthermore, for $(w, w') \in E_3$ and $(u, v), (u', v') \in U \times V$ such that $f(u) = g(v) = w$ and $f(u') = g(v') = w'$, let

$$R((u', v') \mid (u, v)) = \frac{P(u' \mid u) \cdot Q(v' \mid v)}{\mathbb{P}(Z_1 = w' \mid Z_0 = w)}.$$

If $f(u) = g(v) = w$ while (u', v') does not satisfy $f(u') = g(v') = w'$, then let $R((u', v') \mid (u, v)) = 0$. Finally, if $f(u) = g(v) = w$ does not hold, then let $R((u', v') \mid (u, v)) = P(u' \mid u) \cdot Q(v' \mid v)$. Using this definition, one may immediately verify Condition (1), and thus (\tilde{X}, \tilde{Y}) is a transition coupling of X and Y . Furthermore, by construction we have $f(\tilde{X}) = g(\tilde{Y})$ almost surely. \square

With this result in hand, we may now proceed to our second main result concerning factors.

Theorem 18. Let G_1 , G_2 , H_1 , and H_2 be networks with vertex sets U , V , A , and B , and associated Markov chains X , Y , W , and Z , respectively. Suppose that $f : U \rightarrow A$ and $g : V \rightarrow B$ are factor maps from G_1 to H_1 and G_2 to H_2 , and that there are cost functions $c_{ext} : U \times V \rightarrow \mathbb{R}_+$ and $c : A \times B \rightarrow \mathbb{R}_+$ such that $c_{ext}(u, v) = c(f(u), g(v))$.

1. If (\tilde{X}, \tilde{Y}) is an optimal transition coupling of X and Y with respect to c_{ext} , then $(f(\tilde{X}), g(\tilde{Y}))$ is an optimal transition coupling of W and Z with respect to c .
2. If (\tilde{W}, \tilde{Z}) is an optimal transition coupling of W and Z with respect to c , then there exists an optimal transition coupling (\tilde{X}, \tilde{Y}) of X and Y with respect to c_{ext} such that $(f(\tilde{X}), g(\tilde{Y})) \stackrel{d}{=} (\tilde{W}, \tilde{Z})$.

Proof. Let (\tilde{X}, \tilde{Y}) be a transition coupling of X and Y . Since f and g are factor maps, we see that $(f(\tilde{X}), g(\tilde{Y}))$ is a transition coupling of W and Z . Then by the compatibility condition on the cost function we have

$$\mathbb{E}_{c_{ext}}(\tilde{X}, \tilde{Y}) = \mathbb{E}_c(f(\tilde{X}), g(\tilde{Y})). \quad (8)$$

To ease the notational burden of the following argument, we do not distinguish between different couplings of the same random variables. In particular, the notation \tilde{X} may represent formally distinct random variables (defined on different probability spaces) from one instance to the next, although it always denotes a random variable that is equal in distribution to X .

Now let (\tilde{W}, \tilde{Z}) be a transition coupling of W and Z . We claim that there exists a transition coupling (\tilde{X}, \tilde{Y}) such that $(f(\tilde{X}), g(\tilde{Y})) \stackrel{d}{=} (\tilde{W}, \tilde{Z})$. To exhibit the desired transition coupling, we repeatedly use Proposition 19. Let $(\tilde{X}, \tilde{W}, \tilde{Z})$ denote the relatively independent joining of $(X, f(X))$ and (\tilde{W}, \tilde{Z}) over W (with the factor maps given by the natural projections of $(X, f(X))$ onto $f(X) \stackrel{d}{=} W$ and of (\tilde{W}, \tilde{Z}) onto $\tilde{W} \stackrel{d}{=} W$, respectively). Similarly, let $(\tilde{W}, \tilde{Z}, \tilde{Y})$ be the relatively independent joining of (\tilde{W}, \tilde{Z}) and $(g(Y), Y)$ over Z . Now let $(\tilde{X}, \tilde{Y}, \tilde{W}, \tilde{Z})$ be the relatively independent joining of $(\tilde{X}, \tilde{W}, \tilde{Z})$ and $(\tilde{W}, \tilde{Z}, \tilde{Y})$ over (\tilde{W}, \tilde{Z}) . Then the projection of $(\tilde{X}, \tilde{Y}, \tilde{W}, \tilde{Z})$ onto the first two coordinates gives a transition coupling of X and Y with the property that $(f(\tilde{X}), g(\tilde{Y})) \stackrel{d}{=} (\tilde{W}, \tilde{Z})$. We have thus established that every transition coupling (\tilde{W}, \tilde{Z}) of W and Z can be written as $(f(\tilde{X}), g(\tilde{Y}))$ for some transition coupling (\tilde{X}, \tilde{Y}) of X and Y .

The two conclusions of the theorem are immediate consequences of (8) and the result of the previous paragraph. \square

Acknowledgments

KO and ABN were supported in part by NSF grants DMS-1613072 and DMS-1613261. KM gratefully acknowledges the support of NSF CAREER grant DMS-1847144. BY, KM, and ABN would like to acknowledge the support of NSF DMS-2113676.

Appendix A Experimental Details

In this appendix, we provide further details for the experiments discussed in Section 6.

A.1 Network Classification

In order to compute approximate solutions to the NetOTC problem, we used the `EntropicOTC` algorithm [64] with $L = 10$, $T = 50$, $\xi = 100$, and 50 Sinkhorn iterations. The FGW cost was computed with a default parameter choice of $\alpha = 0.5$. The experiment was run on Matlab and a 24-core node in a university-owned computing cluster.

A.2 Network Isomorphism

The classes of networks we dealt with in this experiment are as follows. We give details on how we generated the random networks.

- **SBM:** A description of an SBM is provided in Section 6.4. The given set informs the number of vertices in each block. For example, $\text{SBM}(7,7,7,7)$ indicates an SBM having 4 blocks with 7 vertices in each block. $\text{SBM}(10,8,6)$ has 3 blocks, and each block has 10, 8, and 6 vertices. The connection probabilities within the block were fixed to 0.7, and the probabilities between blocks were 0.1.
- **Erdos-Renyi network:** Erdos-Renyi network is a random network in which every pair of vertices is connected with an independent probability p by an unweighted edge. Remark that the Erdos-Renyi network is equivalent to an SBM with a single block. For each network generation, the number of vertices was randomly determined from the given set. The connection probability p was fixed as given in each class.
- **Random weighted adjacency matrix:** Each element of the adjacency matrix is randomly sampled from the given set. For example, random weighted adjacency matrix $\{0, 1, 2\}$ indicates a network that its adjacency matrix elements are all sampled from the set $\{0, 1, 2\}$. In order to restrict the network to an undirected network, we only sample the upper triangular matrix and the lower triangular matrix is symmetrically filled. Note that the number of vertices is randomly determined between 6 and 20.
- **Random Lollipop network:** An example of a lollipop network is presented in Figure 5. A lollipop consists of a candy part and a stick part. The number of vertices in the candy part is randomly chosen between 7 and 15. The number of vertices in the stick part is also determined between 7 and 15. We also add edges inside the candy to vary the lollipop. With a probability of 0.5, we connect an edge between pair of vertices in the candy. Thus, the candy part will be equivalent to an Erdos-Renyi network.

We discuss how we establish if the algorithm successfully detected isomorphism. For given two isomorphic networks $G_1 = (U, E_1, w_1)$ and $G_2 = (V, E_2, w_2)$, each algorithm returns an vertex alignment $\pi_v : (U, V) \rightarrow [0, 1]$. Define a hard alignment function $\psi(\cdot) = \operatorname{argmax}_{v \in V} \pi(\cdot, v)$, where $\psi : U \rightarrow V$ returns the most aligned vertex in G_2 for each vertex in G_1 . If ψ satisfies the following conditions, the algorithm correctly detects the isomorphism.

1. ψ is bijective.
2. For every $(u_1, u_2) \in E_1$, $(\psi(u_1), \psi(u_2)) \in E_2$ and $w_2(\psi(u_1), \psi(u_2)) = w_1(u_1, u_2)$.
3. For every $(v_1, v_2) \in E_2$, $(\psi^{-1}(v_1), \psi^{-1}(v_2)) \in E_1$ and $w_1(\psi^{-1}(v_1), \psi^{-1}(v_2)) = w_2(v_1, v_2)$.

Figure 8 shows an additional example of detecting network isomorphism. As in Figure 5, NetOTC successfully detects isomorphism, while OT and FGW do not.

The `ExactOTC` algorithm [64] was utilized to solve the NetOTC problem, and a fixed $\alpha = 0.5$ was used for FGW. Note that the algorithms were applied only to the connected network among the generated networks. 95.48% of the generated networks were connected on average. The experiment was developed in Matlab and run on a 24-core node in a university-owned computing cluster.

A.3 Stochastic Block Model Alignment

Cross validation was performed for FGW (to select $\alpha \in \{0, 0.1, \dots, 1\}$) by randomly generating 10 pairs of SBM networks and computing alignments of vertices and edges. Parameters that yielded the highest average alignment accuracy were selected, where separate parameters were chosen for optimizing vertex and edge alignment. 0.1 and 1 were selected for vertex and edge alignment, respectively. We note that this implies GW and FGW were

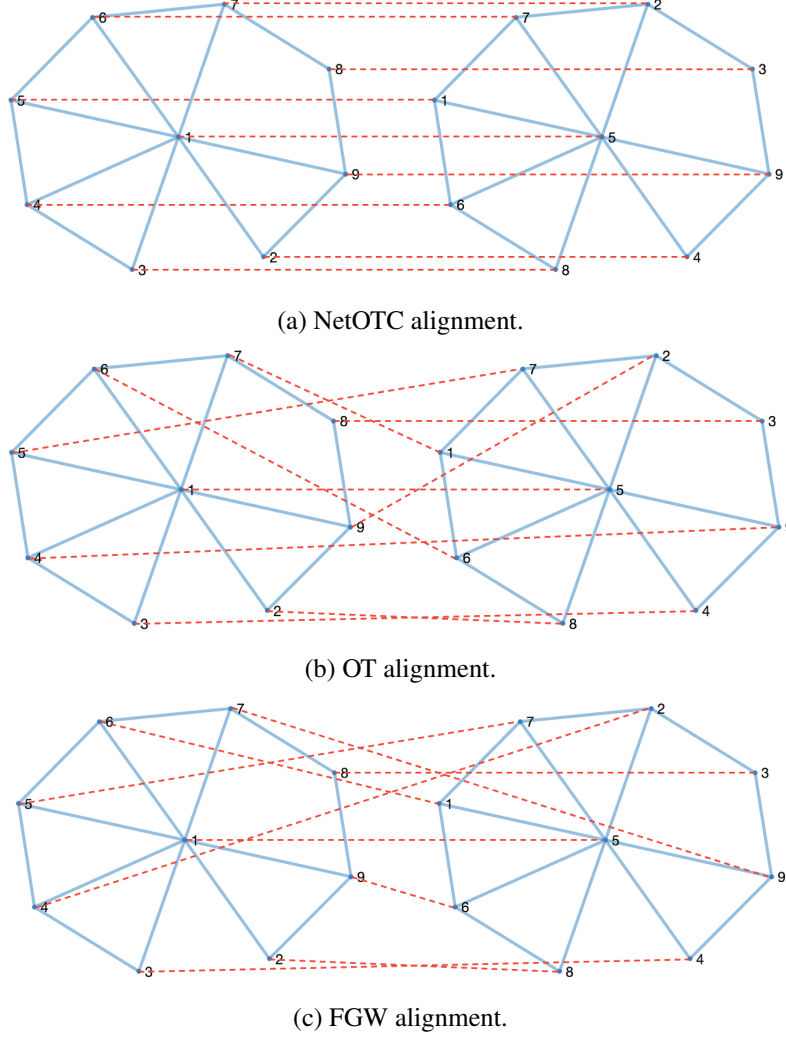


Figure 8: Alignment of two isomorphic wheel networks obtained by NetOTC, OT, and FGW. To make the task challenging, two edges were removed.

equivalent for edge alignment in our experiment. The `ExactOTC` algorithm [64] was used to compute solutions to the NetOTC problem. The experiment was developed and run in Matlab on a personal machine.

A.4 Network Factors

Network G_2 has b vertices embedded in \mathbb{R}^5 where the vertices are sampled from $\mathcal{N}_5(0, \sigma^2 \mathbf{I}_5)$. We denote the vertices of G_2 as V_1, \dots, V_b . Then, we sample m points from $\mathcal{N}_5(V_i, \mathbf{I}_5)$ for each $i = 1, \dots, b$ and the points will be the vertices of G_1 . The total number of vertices of G_1 is bm . We set $b = 6$ and $m = 5$ in this experiment. We used $\alpha = 0.5$ as a default trade-off parameter when applying FGW. As we mentioned in the last paragraph of Section 6.5, the choice of $\alpha \in \{0, 0.1, \dots, 1\}$ doesn't affect the alignment result much.

This experiment was conducted not only in exact factor situations but also when we have approximate factors. We call it an approximate factor when Definition 11 approximately holds as follows. For every $v, v' \in V$ and a given error rate $\epsilon > 0$,

$$\sum_{u' \in f^{-1}(v')} w_1(u, u') \in \left[(1 - \epsilon) \frac{d_1(u)}{d_2(v)} w_2(v, v'), (1 + \epsilon) \frac{d_1(u)}{d_2(v)} w_2(v, v') \right], \quad \forall u \in f^{-1}(v),$$

and

$$\sum_{u \in f^{-1}(v)} \sum_{u' \in f^{-1}(v')} w_1(u, u') = \sum_{u \in f^{-1}(v)} \frac{d_1(u)}{d_2(v)} w_2(v, v').$$

	Exact factor	Approximate factor
	NetOTC	NetOTC
$\sigma = 2.5$	100.00 \pm 0.00	97.94 \pm 0.26
$\sigma = 2.0$	99.91 \pm 0.65	97.57 \pm 1.03
$\sigma = 1.5$	97.46 \pm 4.84	95.87 \pm 3.37
$\sigma = 1.0$	84.09 \pm 11.02	84.06 \pm 11.07

Table 5: Directed networks: alignment accuracies of network factors. Average accuracies observed over 100 random network factors are reported along with their standard deviation.

In particular, we allowed 5% error ($\epsilon = 0.05$) for the second condition in this experiment.

Table 5 reports the vertex alignment accuracy of NetOTC for directed networks at various variance settings. We may check that the performances are similar to applying NetOTC to undirected factor network pairs. Similar to the Stochastic Block Model Alignment experiment, the `ExactOTC` algorithm [64] was used to obtain solutions to the NetOTC problem and was run in Matlab on a personal machine.

References

- [1] E. Abbe. Community detection and stochastic block models: Recent developments. *Journal of Machine Learning Research*, 18(177):1–86, 2018.
- [2] E. Abbe and C. Sandon. Community detection in general stochastic block models: Fundamental limits and efficient algorithms for recovery. *2015 IEEE 56th Annual Symposium on Foundations of Computer Science*, pages 670–688, 2015.
- [3] D. Alvarez-Melis and T. Jaakkola. Gromov-Wasserstein alignment of word embedding spaces. In *Conference on Empirical Methods in Natural Language Processing*, pages 1881–1890, 2018.
- [4] L. Babai. Graph isomorphism in quasipolynomial time. *ArXiv*, abs/1512.03547, 2015.
- [5] X. Bai, X. Bai, J. Cheng, and E. Hancock. *Graph-Based Methods in Computer Vision: Developments and Applications*. IGI Global, USA, 1st edition, 2012.
- [6] B. Barak, C.-N. Chou, Z. Lei, T. Schramm, and Y. Sheng. (Nearly) Efficient Algorithms for the Graph Matching Problem on Correlated Random Graphs. In *NeurIPS*, 2019.
- [7] A. Barbe, M. Sebban, P. Gonçalves, P. Borgnat, and R. Gribonval. Graph diffusion Wasserstein distances. In *European Conference on Machine Learning and Principles and Practice of Knowledge Discovery in Databases*, 2020.
- [8] M. Belkin and P. Niyogi. Laplacian eigenmaps for dimensionality reduction and data representation. *Neural Computation*, 15(6):1373–1396, 2003.
- [9] L. Chen, Z. Gan, Y. Cheng, L. Li, L. Carin, and J. Liu. Graph optimal transport for cross-domain alignment. In *International Conference on Machine Learning*, pages 1542–1553. PMLR, 2020.
- [10] M. Cho, J. Lee, and K. M. Lee. Reweighted random walks for graph matching. In K. Daniilidis, P. Maragos, and N. Paragios, editors, *Computer Vision – ECCV 2010*, pages 492–505, Berlin, Heidelberg, 2010. Springer Berlin Heidelberg.
- [11] D. Conte, P. Foggia, C. Sansone, and M. Vento. Thirty years of graph matching in pattern recognition. *Int. J. Pattern Recognit. Artif. Intell.*, 18:265–298, 2004.
- [12] L. P. Cordella, P. Foggia, C. Sansone, and M. Vento. A (sub)graph isomorphism algorithm for matching large graphs. *IEEE Transactions on Pattern Analysis and Machine Intelligence*, 26:1367–1372, 2004.
- [13] T. Cour, P. Srinivasan, and J. Shi. Balanced graph matching. In *Advances in Neural Information Processing Systems*, volume 19, 2007.
- [14] D. Cullina and N. Kiyavash. Exact alignment recovery for correlated Erdos Renyi graphs. *ArXiv*, abs/1711.06783, 2017.

- [15] D. Cullina, N. Kiyavash, P. Mittal, and H. V. Poor. Partial Recovery of Erdős-Rényi Graph Alignment via k-Core Alignment. *Abstracts of the 2020 SIGMETRICS/Performance Joint International Conference on Measurement and Modeling of Computer Systems*, 2020.
- [16] T. De La Rue. An introduction to joinings in ergodic theory. *arXiv preprint math/0507429*, 2005.
- [17] T. de la Rue. Joinings in ergodic theory. In *Encyclopedia of Complexity and Systems Science*. Springer, New York, NY, 2009.
- [18] A. K. Debnath, R. L. Lopez de Compadre, G. Debnath, A. J. Shusterman, and C. Hansch. Structure-activity relationship of mutagenic aromatic and heteroaromatic nitro compounds. correlation with molecular orbital energies and hydrophobicity. *Journal of Medicinal Chemistry*, 34(2):786–797, 1991.
- [19] P. Demetci, R. Santorella, B. Sandstede, W. S. Noble, and R. Singh. Gromov-Wasserstein optimal transport to align single-cell multi-omics data. *BioRxiv*, 2020.
- [20] J. Ding, Z. Ma, Y. Wu, and J. Xu. Efficient random graph matching via degree profiles. *Probability Theory and Related Fields*, 179:29–115, 2020.
- [21] Y. Dong and W. Sawin. COPT: Coordinated optimal transport on graphs. In *Advances in Neural Information Processing Systems*, 2020.
- [22] M. H. Ellis. The \bar{d} -distance between two Markov processes cannot always be attained by a Markov joining. *Israel Journal of Mathematics*, 24(3-4):269–273, 1976.
- [23] M. H. Ellis. Distances between two-state Markov processes attainable by Markov joinings. *Transactions of the American Mathematical Society*, 241:129–153, 1978.
- [24] M. H. Ellis. On Kamae’s conjecture concerning the d-distance between two-state Markov processes. *The Annals of Probability*, pages 372–376, 1980.
- [25] M. H. Ellis et al. Conditions for attaining \bar{d} by a Markovian joining. *The Annals of Probability*, 8(3):431–440, 1980.
- [26] A. Elmsallati, C. Clark, and J. K. Kalita. Global alignment of protein-protein interaction networks: A survey. *IEEE/ACM Transactions on Computational Biology and Bioinformatics*, 13:689–705, 2016.
- [27] O. Enqvist, K. Josephson, and F. Kahl. Optimal correspondences from pairwise constraints. In *2009 IEEE 12th International Conference on Computer Vision*, pages 1295–1302, 09 2009.
- [28] S. Feizi, G. T. Quon, M. Recamonde-Mendoza, M. Médard, M. Kellis, and A. Jadbabaie. Spectral alignment of graphs. *IEEE Transactions on Network Science and Engineering*, 7:1182–1197, 2020.
- [29] H. Furstenberg. Disjointness in ergodic theory, minimal sets, and a problem in diophantine approximation. *Theory of Computing Systems*, 1(1):1–49, 1967.
- [30] M. R. Garey and D. S. Johnson. *Computers and Intractability; A Guide to the Theory of NP-Completeness*. W. H. Freeman & Co., 1990.
- [31] E. Glasner. *Ergodic Theory via Joinings*, volume 101. American Mathematical Society, 2003.
- [32] S. Gold and A. Rangarajan. A graduated assignment algorithm for graph matching. *IEEE Transactions on Pattern Analysis and Machine Intelligence*, 18:377 – 388, 05 1996.
- [33] R. M. Gray, D. L. Neuhoff, and P. C. Shields. A generalization of Ornstein’s \bar{d} distance with applications to information theory. *The Annals of Probability*, pages 315–328, 1975.
- [34] A. Grover and J. Leskovec. node2vec: Scalable feature learning for networks. *Proceedings of the 22nd ACM SIGKDD International Conference on Knowledge Discovery and Data Mining*, 2016.
- [35] W. L. Hamilton. Graph representation learning. *Synthesis Lectures on Artificial Intelligence and Machine Learning*, 14(3):1–159, 2020.
- [36] P. W. Holland, K. B. Laskey, and S. Leinhardt. Stochastic blockmodels: First steps. *Social Networks*, 5:109–137, 1983.
- [37] R. A. Howard. *Dynamic Programming and Markov Processes*. John Wiley, 1960.
- [38] B. Jiang, J. Tang, C. Ding, Y. Gong, and B. Luo. Graph matching via multiplicative update algorithm. In *Advances in Neural Information Processing Systems*, volume 30, 2017.

- [39] M. Kalaev, V. Bafna, and R. Sharan. Fast and accurate alignment of multiple protein networks. *Journal of computational biology : a journal of computational molecular cell biology*, 16 8:989–99, 2008.
- [40] E. Kazemi, S. H. Hassani, M. Grossglauser, and H. P. Modarres. PROPER: global protein interaction network alignment through percolation matching. *BMC Bioinformatics*, 17, 2016.
- [41] B. P. Kelley, R. Sharan, R. M. Karp, T. Sittler, D. E. Root, B. R. Stockwell, and T. Ideker. Conserved pathways within bacteria and yeast as revealed by global protein network alignment. *Proceedings of the National Academy of Sciences of the United States of America*, 100:11394 – 11399, 2003.
- [42] B. P. Kelley, B. Yuan, F. I. Lewitter, R. Sharan, B. R. Stockwell, and T. Ideker. PathBLAST: a tool for alignment of protein interaction networks. *Nucleic acids research*, 32 Web Server issue:W83–8, 2004.
- [43] K. Kersting, N. M. Kriege, C. Morris, P. Mutzel, and M. Neumann. Benchmark data sets for graph kernels, 2016. <http://graphkernels.cs.tu-dortmund.de>.
- [44] G. W. Klau. A new graph-based method for pairwise global network alignment. *BMC Bioinformatics*, 10:S59 – S59, 2009.
- [45] N. Korula and S. Lattanzi. An efficient reconciliation algorithm for social networks. *ArXiv*, abs/1307.1690, 2014.
- [46] N. M. Kriege, M. Fey, D. Fisseler, P. Mutzel, and F. Weichert. Recognizing Cuneiform signs using graph based methods. In *International Workshop on Cost-Sensitive Learning*, pages 31–44. PMLR, 2018.
- [47] O. Kuchaiev, T. Milenković, V. Memisevic, W. B. Hayes, and N. Przulj. Topological network alignment uncovers biological function and phylogeny. *Journal of The Royal Society Interface*, 7:1341 – 1354, 2010.
- [48] O. Kuchaiev and N. Przulj. Integrative network alignment reveals large regions of global network similarity in yeast and human. *Bioinformatics*, 27 10:1390–6, 2011.
- [49] C. Lee and D. Wilkinson. A review of stochastic block models and extensions for graph clustering. *Applied Network Science*, 4:1–50, 2019.
- [50] M. Leordeanu and M. Hebert. A spectral technique for correspondence problems using pairwise constraints. In *IEEE International Conference on Computer Vision*, volume 2, pages 1482–1489 Vol. 2, 2005.
- [51] M. Leordeanu, M. Hebert, and R. Sukthankar. An integer projected fixed point method for graph matching and map inference. In *Advances in Neural Information Processing Systems*, volume 22, 2009.
- [52] D. A. Levin and Y. Peres. *Markov Chains and Mixing Times*, volume 107. American Mathematical Soc., 2017.
- [53] O. Lezoray and L. Grady. *Image Processing and Analysis with Graphs: Theory and Practice*. Digital Imaging and Computer Vision. CRC Press, 2012.
- [54] D. Lind and B. Marcus. *An Introduction to Symbolic Dynamics and Coding*. Cambridge University Press, 1995.
- [55] E. Loiola, N. Abreu, P. Boaventura-Netto, P. Hahn, and T. Querido. A survey of the quadratic assignment problem. *European Journal of Operational Research*, 176:657–690, 01 2007.
- [56] V. Lyzinski, D. E. Fishkind, and C. E. Priebe. Seeded graph matching for correlated Erdős-Rényi graphs. *J. Mach. Learn. Res.*, 15:3513–3540, 2014.
- [57] H. P. Maretic, M. E. Gheche, G. Chierchia, and P. Frossard. GOT: An Optimal Transport framework for Graph comparison. In *Advances in Neural Information Processing Systems*, 2019.
- [58] H. P. Maretic, M. E. Gheche, M. Minder, G. Chierchia, and P. Frossard. Wasserstein-based graph alignment. *arXiv preprint arXiv:2003.06048*, 2020.
- [59] B. D. McKay and A. Piperno. Practical graph isomorphism, ii. *J. Symb. Comput.*, 60:94–112, 2014.
- [60] F. Mémoli. Gromov–Wasserstein distances and the metric approach to object matching. *Foundations of Computational Mathematics*, 11(4):417–487, 2011.
- [61] A. Narayanan and V. Shmatikov. Robust de-anonymization of large sparse datasets. In *2008 IEEE Symposium on Security and Privacy (sp 2008)*, pages 111–125, 2008.

- [62] A. Narayanan and V. Shmatikov. De-anonymizing social networks. In *2009 30th IEEE Symposium on Security and Privacy*, pages 173–187, 2009.
- [63] K. O’Connor, K. McGoff, and A. B. Nobel. Estimation of stationary optimal transport plans. *arXiv preprint arXiv:2107.11858*, 2021.
- [64] K. O’Connor, K. McGoff, and A. B. Nobel. Optimal transport for stationary Markov chains via policy iteration. *Journal of Machine Learning Research*, 23(45):1–52, 2022.
- [65] D. S. Ornstein. An application of ergodic theory to probability theory. *The Annals of Probability*, 1(1):43–58, 1973.
- [66] B. Perozzi, R. Al-Rfou, and S. Skiena. DeepWalk: online learning of social representations. *Proceedings of the 20th ACM SIGKDD international conference on Knowledge discovery and data mining*, 2014.
- [67] G. Peyré and M. Cuturi. *Computational Optimal Transport*. Now Publishers, Inc., 2019.
- [68] G. Peyré, M. Cuturi, and J. Solomon. Gromov-Wasserstein averaging of kernel and distance matrices. In *International Conference on Machine Learning*, pages 2664–2672. PMLR, 2016.
- [69] M. D. Plummer. Graph factors and factorization: 1985–2003: a survey. *Discrete Mathematics*, 307(7-8):791–821, 2007.
- [70] J. Qian, X. Li, C. Zhang, and L. Chen. De-anonymizing social networks and inferring private attributes using knowledge graphs. *IEEE INFOCOM 2016 - The 35th Annual IEEE International Conference on Computer Communications*, pages 1–9, 2016.
- [71] K. Riesen and H. Bunke. IAM graph database repository for graph based pattern recognition and machine learning. In *Joint International Workshops on Statistical Techniques in Pattern Recognition and Structural and Syntactic Pattern Recognition*, pages 287–297. Springer, 2008.
- [72] C. Schellewald and C. Schnörr. Probabilistic subgraph matching based on convex relaxation. In *Energy Minimization Methods in Computer Vision and Pattern Recognition*, pages 171–186, Berlin, Heidelberg, 2005. Springer Berlin Heidelberg.
- [73] R. Singh, J. Xu, and B. Berger. Global alignment of multiple protein interaction networks with application to functional orthology detection. *Proceedings of the National Academy of Sciences*, 105(35):12763–12768, 2008.
- [74] J. Song, Y. Gao, H. Wang, and B. An. Measuring the distance between finite Markov decision processes. In *Proceedings of the 2016 international conference on autonomous agents & multiagent systems*, pages 468–476. International Foundation for Autonomous Agents and Multiagent Systems, 2016.
- [75] J. J. Sutherland, L. A. O’Brien, and D. F. Weaver. Spline-fitting with a genetic algorithm: A method for developing classification structure- activity relationships. *Journal of Chemical Information and Computer Sciences*, 43(6):1906–1915, 2003.
- [76] V. Titouan, N. Courty, R. Tavenard, and R. Flamary. Optimal transport for structured data with application on graphs. In *International Conference on Machine Learning*, pages 6275–6284, 2019.
- [77] H. Toivonen, F. Zhou, A. Hartikainen, and A. Hinkka. Compression of weighted graphs. In *International Conference on Knowledge Discovery and Data Mining*, pages 965–973, 2011.
- [78] P. H. S. Torr. Solving Markov Random Fields using Semi Definite Programming. *AI & Society*, 2003.
- [79] B. van Wyk and M. van Wyk. A POCS-based graph matching algorithm. *IEEE Transactions on Pattern Analysis and Machine Intelligence*, 26(11):1526–1530, 2004.
- [80] T. Vayer, L. Chapel, R. Flamary, R. Tavenard, and N. Courty. Fused Gromov-Wasserstein distance for structured objects. *Algorithms*, 13(9):212, 2020.
- [81] T. Vayer, R. Flamary, R. Tavenard, L. Chapel, and N. Courty. Sliced Gromov-Wasserstein. In *Advances in Neural Information Processing Systems*, 2019.
- [82] C. Villani. *Optimal Transport: Old and New*, volume 338. Springer-Verlag Berlin Heidelberg, 2008.
- [83] H. Xu, D. Luo, and L. Carin. Scalable Gromov-Wasserstein learning for graph partitioning and matching. In *Advances in Neural Information Processing Systems*, pages 3052–3062, 2019.

- [84] H. Xu, D. Luo, H. Zha, and L. C. Duke. Gromov-Wasserstein learning for graph matching and node embedding. In *International Conference on Machine Learning*, pages 6932–6941, 2019.
- [85] J. Yan, X.-C. Yin, W. Lin, C. Deng, H. Zha, and X. Yang. A short survey of recent advances in graph matching. In *Proceedings of the 2016 ACM on International Conference on Multimedia Retrieval*, pages 167–174, New York, NY, USA, 2016. Association for Computing Machinery.
- [86] X. Yan. <https://sites.cs.ucsb.edu/~xyan/dataset.htm>.
- [87] T. Yao, Y. Pan, Y. Li, and T. Mei. Exploring visual relationship for image captioning. In *ECCV*, 2018.
- [88] L. Yartseva and M. Grossglauser. On the performance of percolation graph matching. In *COSN '13*, 2013.
- [89] T. Yu, J. Yan, Y. Wang, W. Liu, and b. Li. Generalizing graph matching beyond quadratic assignment model. In *Advances in Neural Information Processing Systems*, volume 31. Curran Associates, Inc., 2018.
- [90] M. Zaslavskiy, F. Bach, and J.-P. Vert. A Path Following Algorithm for the Graph Matching Problem. *IEEE Transactions on Pattern Analysis and Machine Intelligence*, 31(12):2227–2242, 2009.
- [91] S. Zhang. Existence and application of optimal Markovian coupling with respect to non-negative lower semi-continuous functions. *Acta Mathematica Sinica*, 16(2):261–270, 2000.
- [92] F. Zhou and F. De la Torre. Factorized graph matching. *IEEE Transactions on Pattern Analysis and Machine Intelligence*, 38(9):1774–1789, 2016.